# Long chain branching on linear polypropylene in the melt by free radical reaction

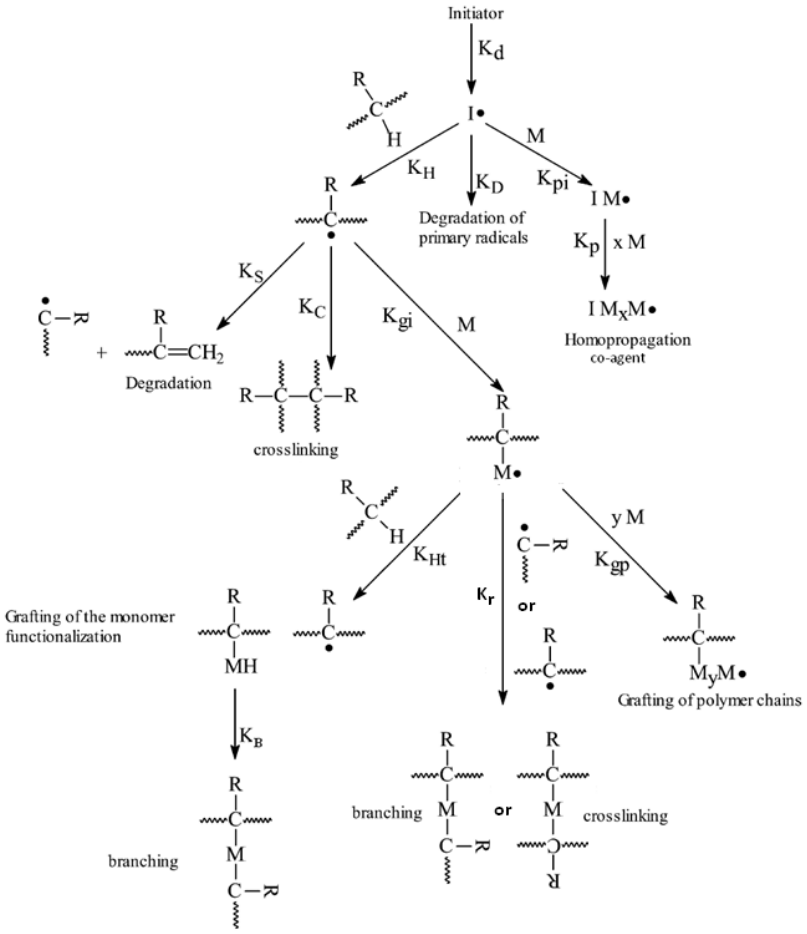


I.C. Goumans
s1703609

Supervisor:
Prof. Dr. F. Picchioni
Prof. A.D. Gotsis

Phd.:
M. Beljaars

Date: 08-06-2013

University of Groningen
Department of Chemical Engineering

# Summary

This thesis describes the research that is performed towards the free radical melt modification of long chain branched (LCB) *isotactic*-Polypropylene (iPP). The synthesis and characterization of LCB-iPP was performed. For reference, chapter 2 captures an overview of the available and useful literature regarding the branching process and the science of rheology.

The synthesis and characterization of LCB-iPP is described in chapter 3. The synthesis was carried out with dicumyl peroxide as free radical initiator and five selected co-agents. The characterization was performed by differential scanning calorimetry (DSC), gel permeation chromatography (GPC) and rheological measurements.

An attempt was made to quantitatively correlate the co-agent properties with the zero shear viscosity, but it was not possible to fit the data in statistically significant way. Nevertheless, at a more qualitative level, few important co-agent properties were defined and a ranking of the use co-agents regarding their ability in inducing long chain branches is presented. It was found that hydroquinone (HQ) resulted in modified iPP with the highest degree of branching while allyl-2-furoate (A2F) was not capable of inducing a branched structure.

Regarding the choice of co-agent, a wide range of different molecules can be used. Many different co-agents which are capable of inducing a branched structure can be found in literature. Various strategies have been proposed to restrain the degradation of iPP and suppress crosslinking during the melt modification. However, to our knowledge, a systematic study towards the choice of co-agent has not been performed yet. This gives rise to the question; what are key features for inducing a branched structure? In this work a systematic study towards the choice of co-agent was performed and few important co-agent properties were defined which can be used for selecting a co-agent.

# Acknowledgements

This report is the result of my graduation project for the completion of my education Chemical Engineering at the University of Groningen. Although the progress of the project didn't go as planned, it was a very useful experience and I enjoyed the time working on it.

There are a few people I would like to thank personally, starting with professor Francesco Picchioni, for his continuously support. His enthusiasm provided me with a lot of energy and motivation. In every discussion, he challenged me to look further and beyond the obvious. I really enjoyed working with him.

I would also like to thank professor Alexandros Gotsis, for all his help and support during my time in Chania, Crete. He put a lot of time and effort in making rheology understandable.

Furthermore, I would like to thank Martijn Beljaars for his support and for ordering all my chemicals. My sincere thanks also go to Gert Alberda, who provided help with the DSC measurements and Andries Jekel for the GPC measurements. And, last but not least, I would like to thank my fellow students for the great atmosphere and the discussions.

# Table of Contents

# 1 Introduction

## 1.1 Long chain branched iPP

Isotactic polypropylene (iPP) is one of the most widely used thermoplastics in the world. This is due to the desirable and beneficial physical properties, such as low density, good heat and chemical resistance, high melting temperature, stiffness and the reusability. Commercial iPP is produced by using metallocene or classical Ziegler-Natta catalytic systems, which results in highly linear chains with a relatively narrow molecular weight distribution. As a consequence, commercial iPP shows low melt strength and weak strain hardening behavior. Many process techniques, like foaming, blow molding, thermoforming, injection molding and spinning, require strain hardening behavior. This can be obtained by introducing long chain branches or broadening the molecular weight distribution. Although the effects of broadening the molecular weight distribution (polydispersity) and long chain branching are pointing in the same direction, the latter is much stronger and more efficient to enhance the melt strength of polymers [1].

So far there are four ways to produce LCB-iPP, through direct synthesis [2] [3], through solid state modification [4], by electron beam irradiation [5] and through melt modification [6] [7] [8] [9] [10] [11] [12] [13] [14] [15] [16] [17] [18] [19] [20].

The direct synthesis of LCB-iPP is carried out using metallocene catalysis directly [21] or via the addition of pre-made iPP macro-monomers [22]. In situ polymerization provides control of the stereochemistry and molecular weight of the LCB-iPP. However, disadvantages of catalytic systems are high costs and reactor fouling.

Another method is the modification by peroxide reactions in the solid state in the presence or absence of a co-agent [4]. The main advantages of this method are restrained β-scission and more control over the process. A disadvantage, however, is the long reaction time which results in low productivity when implemented in industry.

Electron beam irradiation is a popular method because it can be easily used in industry [13]. However, electron beam irradiation produces LCB-iPP with broadened molecular weight distribution and complex branch structures [4].

In this research the modification is carried out in the melt by radical reaction. The major advantages of melt modification are low costs, simple operation and high productivity when implied in industry [13]. However, the melt modification also faces a lot of difficulties due to the many side reactions which make it difficult to control the process. A general scheme of the radical reactions taking place in the modification can be seen in figure 1.

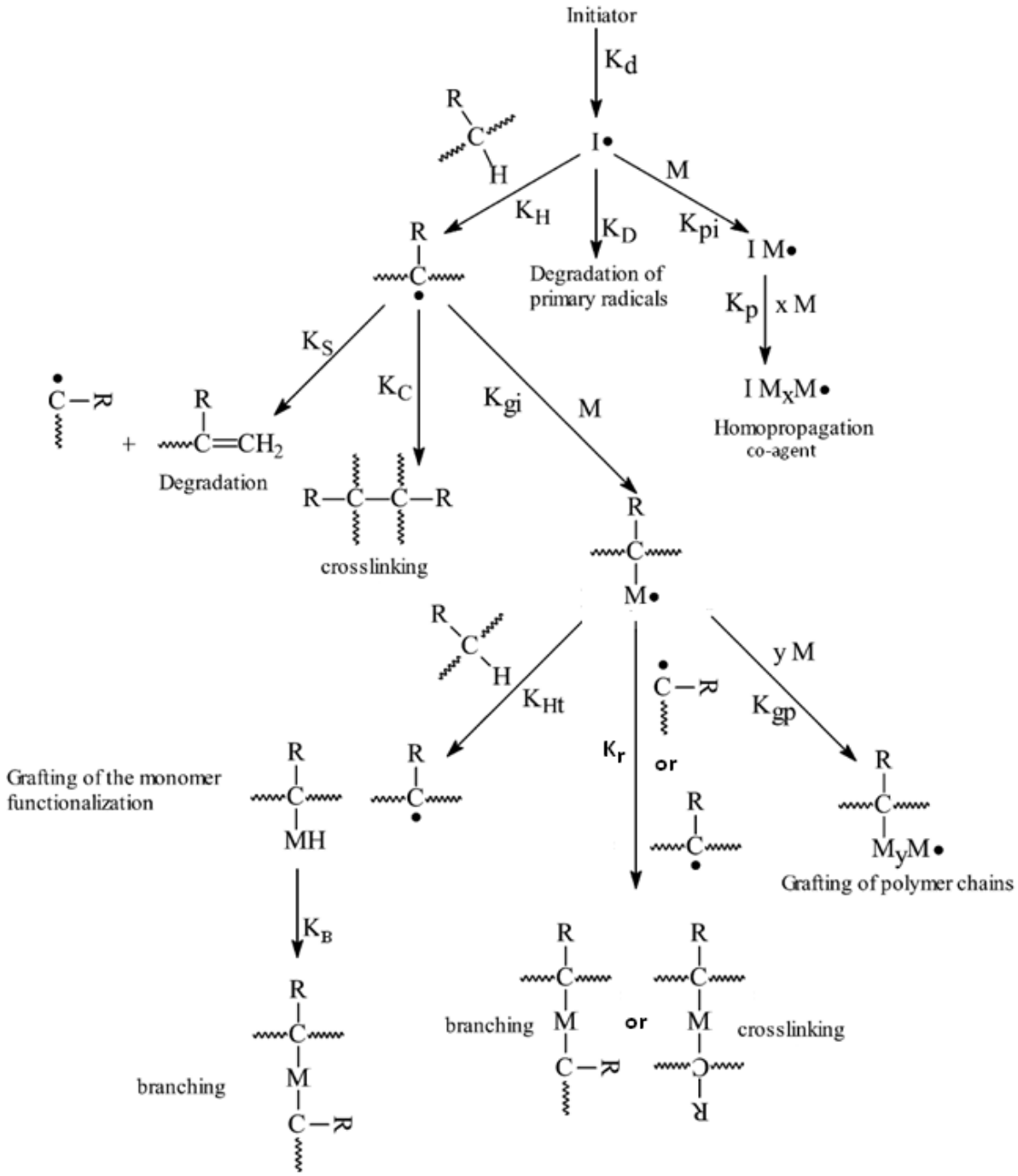


Figure 1: General scheme of the radical reactions (based on [23])

A detailed discussion of this general mechanism will be presented in the following chapters.

## 1.2 Aim and scope

In this thesis isotactic polypropylene (iPP) is modified with long chain branches in the melt through radical reaction. The long chain branches are linked to the iPP backbone with the help of a bi-functional co-agent which acts as a chemical bridge.

A lot of effort in producing branched iPP is performed in the polymer industry and several commercial grades of high melt strength iPP are available [4]. A lot of different co-agents were used for inducing a branched structure to obtain strain hardening behavior. However, to our knowledge, no systematic study towards the choice of co-agent has been performed.

Therefore, the main aim of this thesis is to examine which co-agent is most effective in inducing long chain branches when used in the melt modification and which properties of the co-agent are key features to obtain the desired branched structure. A more accurate understanding of the chemical mechanism involved in the process (co-agent reactions) is required and the factors that have significant influence on the process need to be defined.

The synthesis of the long chain branched (LCB) iPP is carried out through radical melt reaction. The synthesis method is based on existing literature. An overview of the literature is presented in chapter 2. The characterization of the product is performed by differential scanning calorimetry (DSC), gel permeation chromatography (GPC), gel content determination and rheology measurements. DSC, GPC and gel content determination give an indication of the existence of LCB, but rheology measurements are used to verify that long chain branches really exist on the backbone of the chain.

The relevance of this research project is provided in the remainder of this chapter. An overview of the literature on the synthesis and rheology is given in chapter 2. The remainder of this thesis presents the obtained research results.

## 1.3 Relevance

In the last decades, the polymer industry has put a lot of effort in producing branched iPP. The desirable properties of iPP render it one of the most widely used polymers in the world. However, conventional linear iPP has poor melt strength and cannot easily be used in processes where elongational flow is dominant. Unfortunately, there are a lot of industrial situations where there is a large element of extensional flow, such as foaming, blow moulding and spinning. It is therefore expected that the improvement of the elongational flow behavior will substantially contribute to the growth of this polymer in the plastics market [12]. The major advantages of the melt modification are low costs, simple operation and high productivity. It is therefore desirable for the polymer industry to gain more insight and control over the melt process.

# 2 Long chain branched *i*-polypropylene

This chapter gives an overview of available literature on the synthesis and rheology relevant for the remainder of this thesis.

## 2.1 Introduction

Branching and/or crosslinking of polyolefins is usually carried out by the formation of a non-terminal macro-radical, which can recombine with another macro-radical to form the desired structure. The macro-radicals can be produced by hydrogen atom extraction by a radical initiator (peroxide) or through direct scission of the chemical bonds present in the chain structure (ϒ-rays, electron beam) [24]. However, when iPP is treated with a radical initiator it degrades through β-scission. To restrain β-scission, a bi-functional co-agent can be added to the system which reacts with the macro-radical to form a more stable adduct.

The introduction of branches has dramatic effects on the rheological properties of the material in the molten state. More entanglement points are present in LCB-iPP, making the material more elastic. This is mainly measured by a frequency sweep experiment. The branches also give rise to strain hardening behavior which is measured with a controlled strain rate rheometer.

## 2.2 Melt modification

Melt processing of iPP is an attractive synthetic approach to create LCB-iPP. Peroxide initiated chain scission and co-agent assisted linking transforms the architecture of linear iPP into LCB-iPP. The advantages of melt modification lie in the low costs, simple operation and high productivity when implemented in industry. However, melt modification also has his disadvantages; the many side reactions make it difficult to control the process. A general accepted reaction mechanism (with divinylbenzene as co-agent) can be found in figure 2 [4].

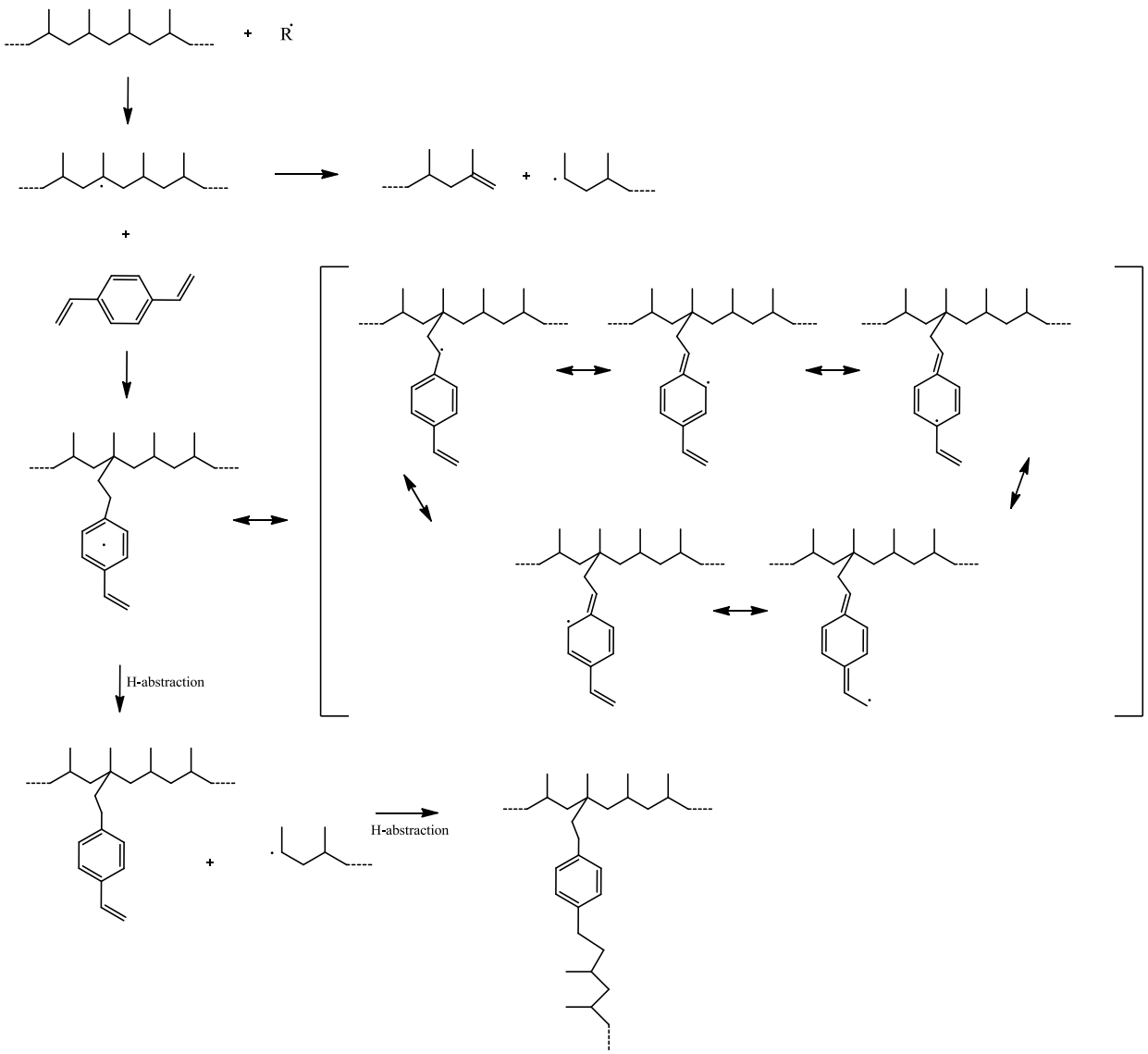


**Figure 2: General accepted reaction mechanism with divinylbenzene as co-agent**

Through decomposition of the peroxide, primary radicals are formed which react with iPP to form macro-radicals. The macro-radicals are not stable and can in principle undergo two main reactions, degradation (β-scission) or stabilization with a co-agent to form the more stable adduct (7). The higher stability of the adduct (7) is provided through the existence of resonance structures. The free radical will abstract a hydrogen from a polypropylene chain forming the grafted adduct (8) which can further react to form the desired long chain branches. At the same time a lot of side reactions are taking place, with crosslinking being the most undesired. The following side reactions can take place [4]:

- Hydrogen abstraction with the initiator instead of the iPP chain
- Direct coupling of two tertiary macro-radicals
- Coupling of the grafted adduct (8) with a tertiary macro-radical

- Homo- and graft- polymerization of the co-agent (initiation by primary radical and macro-radicals respectively)
- Transfer of radical species to the initiator or co-agent

The direct or indirect coupling of tertiary macro-radicals and the direct coupling between two non-terminal macro-radicals leads to the formation of cross-linked polypropylene. To avoid the formation of cross-linked material, β-scission is necessary to ensure that there are enough shorter iPP chains to react with the grafted adduct. This is also demonstrated by blank experiments [25].

Through the years a lot of effort is carried out to control the branching reaction. Various processes are proposed to restrict degradation and prevent crosslinking, like prolonging the lifetime of macro-radicals by reacting with dithiocarbamate radicals reversibly [10] [8] [9] and stabilizing macro-radicals by changing radical intermediate states using styrene [26] or furan derivatives [7]. Unfortunately these methods are not able to fully prevent crosslinking and have little effect on the branching degree. Another drawback, of the above mentioned processes, is that besides a co-agent and peroxide the addition of one more "assisting" agent is necessary to produce the LCB-iPP.

Gotsis and Zeevenhoven [19] used special peroxydicarbonates to synthesize long chain branches on the polypropylene backbone. The peroxydicarbonates used in this research not only provided the radicals in the mixture but also functioned as the chemical bridge (co-agent) between the polypropylene chains. Many more processes have been proposed to produce LCB-iPP. An overview of these processes providing used peroxides and co-agents is given in Appendix A.

Crosslinking and branching are competing reactions. Over the years, a lot of research is performed towards the crosslinking of iPP in the melt through radical reactions (with or without the use of a co-agent). Relevant information about the mechanism, use of co-agent and amount of peroxide used can therefore be found in literature about crosslinking of iPP as well.

### 2.2.1 Factors influencing the process

The control of the final structure is of relevant importance in the synthesis of LCB-iPP. The best process conditions are required to get the desired final structure, limit β-scission and avoid crosslinking. The final structure is determined by reaction parameters such as temperature, co-agent structure, feed composition and duration. A full understanding of the significant influence of these parameters has not been reached yet, but many aspects are under reasonable control and are discussed here.

*Reaction Temperature*

Thermal degradation of the polypropylene chain proceeds by oxidative processes or simply by the action of heat [27]. A higher temperature results in more degraded material and therefore a lower molecular weight. The effect of oxygen (air) on the thermal degradation depends on the mechanisms of polymerization. Beyler and Hirschler [27] state that free radical polymerization leads to neutralization of the effect of oxygen. As a result, less degradation takes place when radicals are presented in the system.

Chodák and Zimányová [28] investigated the effect of temperature on peroxide initiated crosslinking of polypropylene. They observed a decrease of crosslinking efficiency with increasing temperature. These findings support the view that higher temperature increases the rate of fragmentation, due to the higher activation energy of that process, compared with that for macro-radical recombination [29].

*Amount of co-agent and peroxide*

Fragmentation (β-scission) is in principle a first order reaction while recombination (crosslinking) of the macro-radicals is of the second order of magnitude. Therefore a higher amount of macro-radicals in the mixture favors the crosslinking reaction [23] [25] [30].

It is known that radical activity is more intense amongst the largest chains [15]. Therefore the co-agent is preferentially grafted to high molecular weight chains. Furthermore, the grafting of a co-agent onto the polypropylene chain makes the chain more reactive with respect to molecular weight growth [14] and therefore has a more prominent tendency towards crosslinking. Based on these arguments, it can be stated that a cross-linked structure is more likely to occur when a higher amount of co-agent is used.

Last but not least, the reactivity of the co-agent needs to be considered when determining the amount of co-agent and peroxide. A high reactive co-agent requires a lower amount of peroxide for branching to occur while a less reactive co-agent requires a higher amount of peroxide [14].

Coupling of the co-agent and β-scission is required to obtain the desired branched structure. Therefore, the best results are most likely found with a low amount of high reactive co-agent and a low amount of peroxide. These theoretical considerations are in agreement with the results obtained by Wang et al. [6].

*Co-agent structure and reactivity*

Regarding the choice of co-agent, a wide range of different molecules can be used. The selected co-agent needs two double bonds able to react with the formed macro-radicals and at least be bi-functional. Other important properties towards the branching process are solubility in the melt, reactivity of the co-agent, stability of the formed radical and susceptibility towards homo-polymerization.

When the co-agent is not fully soluble in the polypropylene melt, the reaction mainly occurs at the interface and is therefore affected by mixing efficiency and screw design of the extruder [23]. To ensure good solubility of the co-agent in the polypropylene melt, the solubility parameters need to be in the same range.

A co-agent with a high reactivity (towards iPP) grafts relatively fast on the polypropylene chain in comparison with a low reactive co-agent. High reactivity therefore stabilizes the macro-radicals and limits degradation. But according to Parent et al. [15] the grafting increases the capacity for crosslinking, meaning that a high reactivity leads to a cross-linked structure. In order to suppress crosslinking and promote branching, a co-agent with two different reactive double bonds can be used. Zhang et al. [20] demonstrated that the higher reactive double bond preferentially reacts with macro-radicals to stabilize the macro-radicals quickly, while the lower reactive double bond will later react with the secondary radical, formed through β-scission, to avoid the formation of hyper-branched or even cross-linked structure. This method promotes the formation of LCB structure and shows a more uniform distribution of branching and molecular weight.

Furthermore, Chodák et al. [31] stated that the more stable co-agent radical, after recombination with the macro-radicals, leads to a rise of the polymer molecular weight, while a co-agent that is highly reactive towards itself will result in inefficient consumption of the co-agent.

## 2.3 Characterization of the resulting structure

Long chain branches are modified onto the iPP backbone to improve the melt behavior during processing. Characterization of the resulting structure is performed to verify the existence of LCB-iPP. The molecular parameters that are important for the processing properties include the average number of branches per molecule ($B_n$), their topology (the distribution along the chain and their comb- or Cayley tree type structure) and their lengths [4]. There are three main methods to detect the long chain branches, namely nuclear magnetic resonance (NMR), triple sensor gel permeation chromatography (GPC) and rheology measurements, the latter being the most reliable. The first method can detect branches through the resonance peak of the methine carbon. Detection of this methine resonance peak corresponds to branches longer than four carbons [32]. Unfortunately, ordinary NMR isn't capable of detecting the small amount of LCB that is needed for enhancement of the melt strength. Therefore this method is not used in this research. Triple sensor GPC and rheology are discussed below in more detail.

### 2.3.1 Gel permeation chromatography (GPC)

Gel permeation chromatography (GPC) is a type of size-exclusion chromatography that separates the sample on the basis of size. The separation is based on the hydrodynamic volume of the sample, from which one can calculate the molecular mass and its distribution. Branched chains are denser in solution than linear chains of the same molecular weight. Therefore having a lower radius of gyration ($R_g$) and intrinsic viscosity $\eta$ . An estimate of the amount of LCB can be determined from the means square radius of gyration and intrinsic viscosity. The fundament of this method is established by Zimm and Stockmeyer [33]. They expressed the following branching factors:

$$g = \frac{R_{g\ br}^2}{R_{g\ lin}^2} \tag{2.1}$$

$$g' = \frac{\eta_{\ br}}{\eta_{\ lin}} \tag{2.2}$$

Here the captions *br* and *lin* represent branched and linear chains. The relationship of g and g' can be expressed by:

$$g' = g^{\in} \tag{2.3}$$

Here $\in$ takes values between 0.5 and 1.5 [20]. For random branching, a value of 0.75 is often used and from this the average number of branches per polymer, $B_n$, can be calculated, by solving the following equation [12]:

$$g = \left(1 + \frac{B_n}{7} + \frac{4B_n}{9\pi}\right)^{-0.5} \tag{2.4}$$

### 2.3.2 Shear rheology

Polymers show viscoelastic behavior. Typical viscoelastic behavior can be described best with the Burgers model (figure 3). When a force is applied the initial response will be the immediate elastic response ($G_1$). Then there is a delayed elastic response, which can be described as a spring and dashpot in series ($G_2$ and $\eta_2$). The deformation rate here becomes slower and slower until a steady state is reached. This steady state is the viscous response of the model and described by the last dashpot ($\eta_1$). This model shows that the elastic modulus, G, can be described by an immediate elastic response and a delayed elastic response. The immediate solid like response is called the storage modulus, G', the delayed liquid like response is called the loss modulus G''.

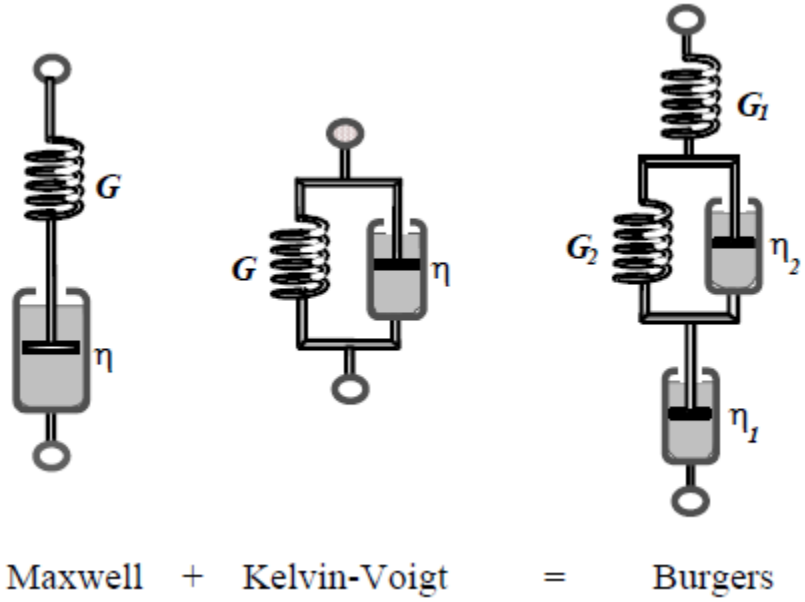


Figure 3: Simple mechanical models describing viscoelastic behavior [34]

Viscoelastic behavior can be analyzed with shear rheology. During an oscillatory test a sine-wave-shaped input of strain, $\gamma$, results in a sinusoidal strain output which can be described as:

$$\gamma = \gamma_0 sin\ \omega t \tag{2.5}$$

Where $\gamma_0$ is the strain amplitude and ω is the angular frequency. The stress can be described in the same way. However, in a viscoelastic material the stress, $\sigma$, is partly damped by the viscous response of the material which results in a shift by a phase angle δ.

$$\sigma = \sigma_0 sin\ \omega t + \delta \tag{2.6}$$

Where $\sigma_0$ is the yield stress. During the shear measurements, the viscoelastic material undergoes an in phase solid like response and a corresponding liquid like response which is π/2 out of phase with the

input [34]. Equation 2.6 can be rewritten by using trigonometry, which results in the following equation [35]:

$$\sigma = \sigma_0 cos\delta \ sin \ \omega t + \sigma_0 sin\delta \ cos \ \omega t = \gamma_0 \ G' sin \ \omega t + G'' cos \ \omega t \quad (2.7)$$

The storage modulus G' and the loss modulus G'' can now be defined as:

$$G' = \frac{\sigma_0}{\gamma_0} cos\delta \quad (2.8)$$

and

$$G'' = \frac{\sigma_0}{\gamma_0} sin\delta \quad (2.9)$$

With the loss tangent:

$$tan\delta = \frac{G''}{G'} \quad (2.10)$$

The G' and G'' produced during the measurements are sometimes reported in different ways, for instance [34]:

$$Dynamic \ viscosity: \eta' = \frac{G''}{\omega} \quad (2.11)$$

$$Complex \ modulus: G^* = \sqrt{G'^2 + G''^2} \quad (2.12)$$

$$Complex \ viscosity: \eta^* = \left(\frac{G'^2}{\omega^2} + \frac{G''^2}{\omega^2}\right)^{\frac{1}{2}} \quad (2.13)$$

From the dynamic viscosity the zero-shear rate viscosity can be estimated by [35]:

$$\lim_{\omega \to 0} \eta' \ \omega = \eta_0 \quad (2.14)$$

The rheology of polymer melts is controlled by molecular weight distribution, degree of branching, temperature and pressure [34]. When additives, such as plasticizers, are used, the concentration is also a factor that controls the rheology. Polymer melts are elastic because tension in the chains between entanglements persists while the entangled chains slide over each other [34]. The onset of entanglements is called the critical molecular weight of the polymer, $M_c$, and this point depends on the chain configuration.

The existence of entanglements makes flow more difficult and therefore the viscosity dramatically increases from the onset of entanglements. This increase in viscosity can be described according to the following equation:

$$\eta_0 = K \ Mw_{av}^{\ 3.4} \quad (2.15)$$

The factors that control the rheology of a polymer melt can often be incorporated into a single master curve by plotting the non-dimensional quantity $\frac{\eta}{\eta_0}$ against $\frac{\eta_0 \gamma Mw^{\alpha}}{\rho T}$, where α is a constant near

unity, $\rho$ is the polymer density at T, the temperature in Kelvin [34]. According to this relation, the broadening of the molecular weight results in a polymer melt behaving non-Newtonian at lower values of shear rate. A similar effect can be seen for the addition of branches onto a polymer backbone. The addition of branches onto a polymer backbone results in a more compact chain (figure 4), this generally results in a lower viscosity in the melt at high shear rates.

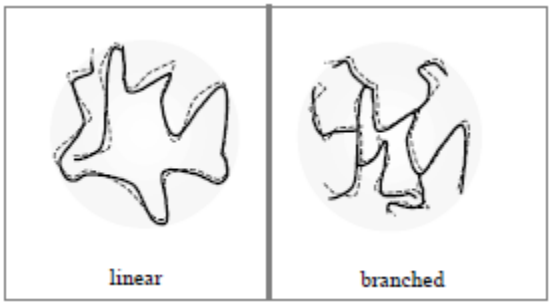


Figure 4: Isolated polymer coils [34]

The addition of long chain branches or broadening the molecular weight increases the possibility for entanglements and thus increases the elasticity. Long chain branches make it difficult for the chains to move at low shear rates and therefore the zero shear viscosity increases, something that is not true for broadening the molecular weight distribution.

According to Tsenoglou and Gotsis [36] this increase in zero shear viscosity, $\eta_0$, can be related to the average number of branches per molecule, $B_n$, with the following equation:

$$B_n \approx \frac{ln\,\frac{\eta_{0,LCB}}{\eta_{0,L}}}{\alpha\,\frac{M_{wl}}{M_c}-1\;-3ln\,\frac{M_{wl}}{M_c}} \tag{2.16}$$

Where $M_{wl}$ is the molecular weight of the linear component, $M_c$= 13640 g/mole for polypropylene [2] and α is a constant independent of the branching point functionality and equal to 15/8 [37] [36]. The molecular weight dependence of the viscosity of the linear component can be described according to the following equation:

$$\eta_l = \eta_c \left(\frac{M_{wl}}{M_c}\right)^{3,4} \tag{2.17}$$

Where $M_c = 2M_e$, with $M_e$ being the molecular weight between two successive entanglements. For PP, $M_e$ is roughly equal to 5600 and $\eta_c$ is the melt viscosity at the entanglement crossover, where $M_{wl} = M_c$ [37]. Now equation 2.16 can be restated as follows:

$$B_n = \frac{ln\,\frac{\eta_{0,LCB}}{\eta_{0,L}}}{\alpha\,\frac{\eta_{0,L}}{\eta_c}\;-1\;-\frac{6}{7}ln\,\frac{\eta_{0,L}}{\eta_c}} \tag{2.18}$$

In order to use this method for determining the long chain branches, the zero shear viscosity, $\eta_0$, needs to be determined. The $\eta_0$ is calculated from the Cross three-parameter fitting equation [38]:

$$\eta^*(\gamma) = \frac{\eta_0}{1 + (\lambda\gamma)^n} \tag{2.19}$$

Where λ is a material constant with units of time and $n$ is related to the power law index. But this method is not so straightforward, because the zero shear viscosity depends on the molar mass as well. It is expected, as discussed earlier, that the viscosity of a linear polymer should follow a 3.4 power-law dependence on molar mass. As a consequence of this, linear polymers with the same $\frac{\eta_0}{M_w^{3.4}}$ value would have about the same viscosity if they had the same $M_w$ [39]. Since the generation of a branched structure in the melt results in different molecular weight of the samples, the zero shear viscosity is normalized, according the following assumption:

$$B_n \propto \frac{\eta_0}{M_w^{3.4}} \tag{2.20}$$

Janzen and Colby [40] proposed a method which even works when the molecular weight changes. In their method, they compare the zero shear viscosity of the linear and the branched polymers. The general behavior observed in branched polymers can be described according to:

$$\eta_0 = AM_b \left(1 + \left(\frac{M_b}{M_c}\right)^{2.4}\right)^{\left(\frac{M_w}{M_b}\right)^{s(\gamma)}} \tag{2.21}$$

Where $M_b$ is an average molecular mass between a branch point and its adjacent vertexes, either chain ends or other branch points, A is a parameter that can be evaluated if $\eta_0$ and $M_w$ of the linear polymer are known and $^s(\gamma)$ is dependent on $M_b$ according to the following equation [40]:

$$^s(\gamma) = max\left(1, \frac{3}{2} + \frac{9}{8}B\ln\left(\frac{M_b}{90M_{Kuhn}}\right)\right) \tag{2.22}$$

Where *B* is a constant and $M_{Kuhn}$ for polypropylene is 187.8 g/mole. It is now possible to determine the value of $M_b$, because $A, B, M_c$ and $M_{Kuhn}$ are known constants and $\eta_0$ and $M_w$ are measured values.

Another indication for branching is given by the relaxation time. The dynamic shear measurements result in curves of the dynamic moduli (G'(ω) and G''(ω)). At low frequencies, G' is lower than G''. The point where G' crosses over G'' is the characteristic relaxation time for het polymer, $t_{cr} = \frac{1}{\omega_{cr}}$. The addition of branches affects G' and G'' and the value of the relaxation time increases with increasing $B_n$. Therefore, longer $t_{cr}$ indicates higher elasticity and, indirectly, more branching [37].

*Time-temperature superposition*

A time-temperature superposition can be done to give additional information about the molecular structure of the polymer. The essence of this time-temperature concept is that if all the relaxation phenomena involved in $G(t)$ have the same temperature dependency, then changing the temperature of a measurement will have the same effect on the data as shifting the data horizontally on the log(time) or log(frequency) axis [41]. The change in temperature from some reference temperature $T_0$ to a different temperature $T$ has the following effect on the relaxation time:

$$\tau_i(T) = a_T(T)\,\tau_i(T_0) \tag{2.23}$$

where $a_T$ is the horizontally shift factor. The dependence of the time shift factor is most commonly described with the Arrhenius dependence or the WLF dependence, which are given below by equation 2.24 and 2.25

$$a_T\ T\ = exp\ \frac{E_a}{R}\ \frac{1}{T} - \frac{1}{T_0} \tag{2.24}$$

$$a_T\ T\ = \frac{-C_1^0\ T-T_0}{C_2^0 +\ T-T_0} \tag{2.25}$$

The Arrhenius dependence is used when the temperature is at least hundred degrees above the glass transition temperature, while the WLF dependence provides a better fit of data at temperatures closer to $T_g$ [41]. A horizontal shift alone is often not sufficient to make the relaxation modulus data measured at $T$ superpose onto the data measured at $T_0$. A vertical shift factor is also required and given by the following definition:

$$b_T = \frac{\rho_0 T_0}{\rho T} \tag{2.26}$$

where $\rho$ is the density. For linear polymers excellent superposition of both G' and G'' can be observed (thermorheological simplicity), while for branched structures superposition for G' is possible while for G'' lack of superposition (dispersion) is observed (thermorheological complex) [42].

*Van Gurp-Palmen Analysis*

The main idea of the Van Gurp-Palmen analysis is to plot the loss angle $\delta = tan^{-1}\ G''/G'$ versus the magnitude of the complex modulus, $G^*$ [42]. A linear polymer has a loss angle close to 90° which indicates viscous behavior of the polymer. The lower the value of δ, the more solid like (elastic) the material is. Obviously, there is no more information in the van Gurp-Palmen plot then in the usual plot of $G'$ and $G''$ versus $\omega$, but this form of presentation shows the LCB features more transparently and therefore gives a good indication for the formation of branches. Another method that gives a good indication of the elasticity of the samples is plotting the loss angle versus the frequency.

### 2.3.3 Extensional rheology

An extensional or elongational flow can be defined as deformation that involves stretching along the streamlines [35]. By stretching the polymer material in one direction it undergoes uniaxial extensional flow (figure 5).

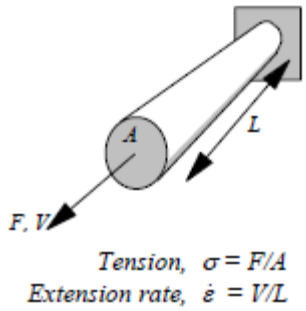


Figure 5: Definition diagram for uniaxial extensional flow [34]

As can be seen in figure 5, a tension (extensional stress) $\sigma_e$ and an extension rate $\varepsilon$ can be defined. Furthermore, with the ratio of the tension and extension rate, the extensional viscosity can be defined:

$$\eta_e = \frac{\sigma_e}{\varepsilon} \tag{2.27}$$

The stress growth during uniaxial elongation of polymeric melts can be described by several viscoelastic models. One of the most successful models is the Rubber-Like Liquid model of Lodge. By assuming separability of time, this model can be modified to account for nonlinear, strain thinning effects by the incorporation of a damping function to the viscoelastic memory [37]:

$$\sigma = \int_{-\infty}^{t} \mu\ t-t'\ h\ \lambda\ F\ t-t'\ dt' \tag{2.28}$$

In this equation, F is the Finger deformation tensor, h(λ) is the damping function, λ is the stretch as a function of present and past time (λ(t,t'), and μ is the memory function. The memory function, μ, is a material function of time and depends on the relaxation of the melt. The damping function, h(λ), physically signifies the extent of the stress loss due to the reduction of the entanglement density of segmental orientation following the deformation of a given magnitude, λ [37].

A simple form for the damping function that accommodates the essential phenomenology, the controlled exponential growth of $\eta_e$, and LCB effects of variable intensity, is the following [37]:

$$h\ \lambda\ = \lambda^{-\beta} \tag{2.29}$$

In this equation β(≥0) is an adjustable parameter that depends on the branching number. Increasing branching number leads to better network connectivity, improved resistance to strain-induced network destruction and, therefore, to less stress damping and smaller β values [37].

The stretch in uniaxial elongational flow at constant strain rate is: $\lambda = e^{\varepsilon} = e^{\varepsilon t}$. The damping function of equation 2.29 then becomes [37]:

$$h\ \lambda\ = e^{\ -\beta\varepsilon\ t-t'} \tag{2.30}$$

With this h(λ) Lodge's Rubber-Like Liquid model with a damping function gives the following for the viscosity growth in uniaxial elongation [37]:

$$\eta_e = \frac{\sigma_{11} - \sigma_{22}}{\varepsilon}$$

$$= 1\varepsilon \int_{-\infty}^{t} \mu\ t - t'\ exp\ -\beta\varepsilon\ t - t'\quad exp\ 2\varepsilon\ t - t'\quad - exp\ -\varepsilon\ t - t'\quad dt' \qquad (2.31)$$

The non-Newtonian behavior of polymer melts lead to extensional thickening or strain hardening, meaning an increase in viscosity at higher extension rates. The branching number can be estimated by directly measuring the strain hardening. The $\eta_e$curves can be fitted by the Lodge's Rubber-Like Liquid model that implements the damping function (equation 2.31). The estimated model parameters are then used to infer the value of $B_n$. Gotsis [37] showed that the parameter β decreases monotonically with the increase of $B_n$. Therefore the value of β can be used as a measure of the degree of branching. An empirical relationship between β and the degree of branching is [37]:

$$\beta_u \approx 2e^{-a^3\ \overline{B_n}} \qquad (2.32)$$

with $a = 2.9$. In other situations it was found that $a = 1.5$, this indicates that a is not a universal constant but depends on the MWD breadth and the details of branching.

There are many every day and industrial situations where there is a large element of extensional flow. When the extensional viscosity is low, the material will fail when used in industrial applications as foaming, blow moulding and spinning. There are two methods to increase the extensional viscosity of the polymer melt, through branching and broadening the molecular weight. Hereby the extensional viscosity will increase with increasing extension rate. The effect of branching can be seen in figure 6, broadening the molecular weight results in the similar strain hardening behavior.

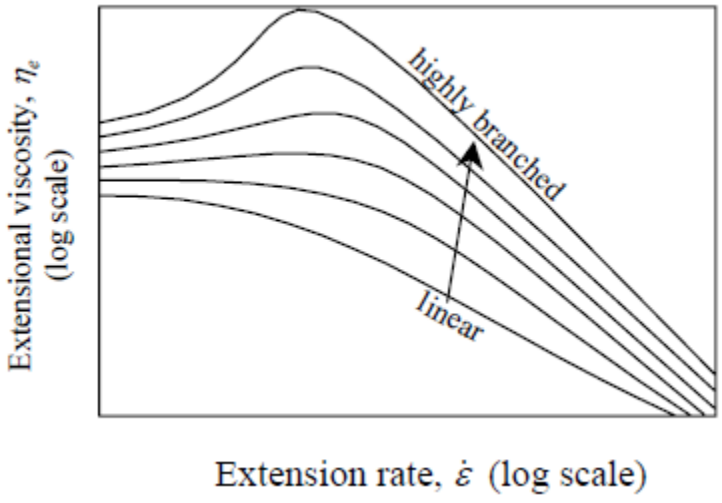


Figure 6: Effect of branching on the extensional viscosity of polymer melts [34]

# 3 Synthesis and characterization of long chain branched *i*-polypropylene

## 3.1 Abstract

Long chain branches (LCB) were added to initially linear isotactic-polypropylene (iPP) in the melt through radical reactions. This was carried out in the presence of a free radical initiator (dicumyl peroxide) and selected co-agents. The modified samples were characterized by differential scanning calorimetry (DSC), gel permeation chromatography (GPC) and rheological measurements. Several properties of a co-agent that have significant influence on the obtained structure were defined. Furthermore, the efficiency of the co-agents was evaluated. Hydroquinone (HQ) resulted in modified iPP with the highest degree of branching while allyl-2-furoate (A2F) was not capable of inducing a branched structure.

## 3.2 Introduction

As noticed in chapter 1 and 2, addition of long chain branches on the iPP backbone significantly improves the process conditions of iPP. The use of LCB-iPP instead of linear iPP enlarges the choice of process techniques. In this report LCB-iPP is produced in the melt through radical reaction. Advantages of producing LCB-iPP in the melt are low cost, simple operation and high productivity; however, one major disadvantage is the difficulty to control the process. The two major side reactions during the process are crosslinking and β-scission. A generally accepted reaction mechanism was already discussed in chapter 2, section 2.2.

There are many factors that have significant influence on the process and the final obtained structure. One of the key factors on the final obtained structure is the used co-agent. A wide range of different co-agents which are capable of inducing a branched structure can be found in existing literature. However, to our knowledge, no systematic study towards the choice of co-agent has been performed. The main aim of this thesis is to evaluate the effectiveness of the several co-agents to induce a branched structure and define properties of the co-agent that have a significant influence on the final structure.

A more accurate understanding of the chemical mechanism involved can give more control over the process and the final structure. Five co-agents were selected in this research and used in combination with dicumyl peroxide (DCP) as radical initiator. The co-agents differ in solubility (in iPP) and reactivity. Their chemical structure, solubility parameter[1], $\delta_s$, and the absolute electronegativity difference (of the reactive bonds)[2], $\Delta e$ , are reported in table 1.

[1] Calculated by the group contribution method

[2] Calculated by HyperChem

The first co-agent used in this research is divinylbenzene. Divinylbenzene is selected since it is quite soluble in iPP and the double bonds can easily react with the free macro-radicals that are formed on the iPP chains. A drawback, however, is that divinylbenzene is a self-polymerisable monomer (more reactive towards itself than towards iPP) and is therefore expected to be susceptible towards crosslinking and/or homo-polymerization. This phenomenon was also observed by other researchers [4] [20].

| Chemical name | Abbreviation | Chemical structure | $\delta_s$ (cal/cm$^3$)$^{0.5}$ | $\Delta e$ |
|---|---|---|---|---|
| Divinylbenzene | DVB | 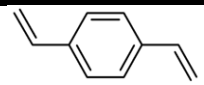 | 8.8 | 0.059 |
| *p*-Benzoquinone | BQ | 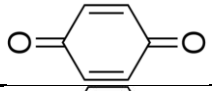 | 12.8 | 0.256 |
| Hydroquinone | HQ | 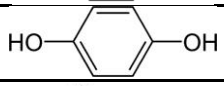 | 15.1 | 0.250 |
| Methyl-*p*-Benzoquinone | MBQ | 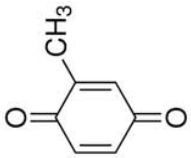 | 11.1 | 0.074<br>0.005 |
| Allyl 2-furoate | A2F | 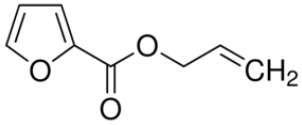 | 10.7 | 0.176<br>0.039 |
| Polypropylene | iPP | - | 7.4 | - |

Table 1: Information about the used chemicals

The second co-agent that was selected is *p*-benzoquinone. *p*-Benzoquinone is highly reactive, but less soluble in iPP in comparison with DVB. A highly reactive co-agent grafts relatively fast on the iPP chain to form the stabilized structure and limits degradation. But according to Parent et al. [14] [15] the grafting of a co-agent onto the polypropylene chain makes the chain more reactive with respect to molecular weight growth and therefore has a more prominent tendency towards crosslinking.

To suppress crosslinking, β-scission is required to ensure that there are enough shorter iPP chains to react with the grafted adduct. The introduction of an induction time ensures β-scission and the thereby corresponding shorter iPP chains. Based on these arguments, the third selected co-agent is hydroquinone. Hydroquinone is not very soluble in iPP, but is highly reactive and a well-known inhibitor [43] capable of "consuming" two radicals (figure 7). Hydroquinone need to be converted into *p*-benzoquinone before it has the desired carbon-carbon double bonds which are required to react with the free macro-radicals on the iPP chain. As a consequence, this gives rise to an induction time. Furthermore, the conversion of hydroquinone to *p*-benzoquinone consumes radicals resulting in a decrease in radicals over time and therefore limiting degradation at the end of the process.

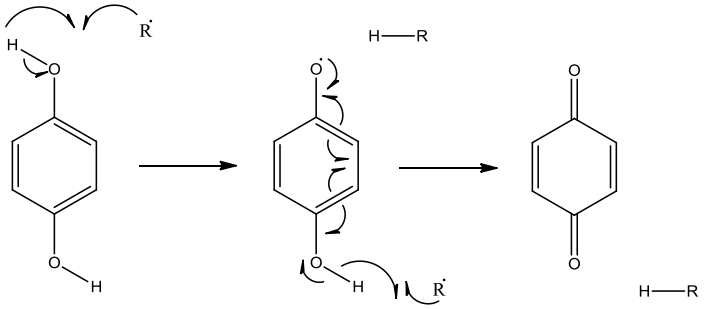

Figure 7: Hydroquinone inhibition mechanism

Another approach is the use of a co-agent with two different kinds of carbon-carbon double bonds. Methyl-*p*-benzoquinone was therefore chosen as the fourth co-agent in this research. The "highly" reactive double bond of methyl-*p*-benzoquinone can react quickly with the free macro-radicals to form the stabilized structure, while the lower reactive double bond can later react with the secondary radical formed through β-scission. This approach results in fast stabilization and a delayed branching reaction. Furthermore, methyl-*p*-benzoquinone has a higher solubility in iPP then *p*-benzoquinone and hydroquinone but is less reactive.

The last selected co-agent is allyl-2-furoate which also has two different kinds of carbon-carbon double bonds, but higher reactivity and solubility in iPP in comparison with methyl-*p*-benzoquinone. However, allyl-2-furoate is a self-polymerisable monomer [44] which, as discussed before, can be a disadvantage and lead to crosslinking and/or homo-polymerization.

This chapter will describe the modification of iPP in the melt through radical reactions and the characterization of the modified material. The characterization of the modified samples was performed by determination of crystallization temperature, molecular weight and gel content. At the end, rheology measurements were used to verify that the LCB really exist on the backbone of the iPP chains.

## 3.3 Experimental

### 3.3.1 Materials

The isotactic polypropylene was supplied by Sabic, Geleen, in powder form with number average molecular weight ($M_n$) of 50,172 g/mol, weight average molecular weight ($M_w$) of 293,013 g/mol and a polydisperisty ($M_w/M_n$) of 5.84. The powder was stored at -17°C since it didn't contain any stabilizer. Divinylbenzene[3] (DVB, Aldrich), hydroquinone (HQ, Aldrich), *p*-benzoquinone (BQ, Aldrich), methyl-p-benzoquinone (MBQ , Aldrich), allyl 2-furoate (A2F, Aldrich), dicumyl peroxide (DCP, Aldrich) and di-tert-butyl p-cresole (BHT, Aldrich) were purchased as high purity products (98%) and were used as received.

### 3.3.2 Preparation of the samples

The reagents, 37 mmol/kg iPP peroxide (DCP) and 0.025-1 wt% (with respect to iPP) co-agent (DVB, HQ, BQ, MBQ or A2F) were dissolved in acetone. Acetone was chosen because it could dissolve the

[3] Purchased with 85% purity

reagents but not the polymer and evaporates easily. Cups with the desired amount of peroxide and co-agents were made. Ten gram of iPP was introduced into a Brabender® batch mixer at a temperature of 170°C (5 half times of DCP decomposition[4]) and a mixing speed of 60 rpm. After 4 minutes at the said temperature, the co-agent was added with a pipette to the melted polymer. After 2 minutes from the addition of the co-agent, peroxide was added with a pipette. After 8 minutes from the addition of the peroxide 0.2 gram of stabilizer (BHT) was added. After 1 minute from the addition of BHT the Brabender was turned off and the polymer melt was removed from the Brabender. All the samples are prepared following this procedure.

### 3.3.3 Thermal behavior, molecular weight and gel content determination

Differential scanning calorimetry (DSC) was used to determine the crystallization temperature of the samples. The specimens were heated to 200°C at a rate of 10°C/min and remained at 200°C for 5 minutes to eliminate the thermal histories and then cooled down to -50°C with a rate of 10°C/min to determine the crystallization temperature. Then the samples were reheated ones more from -50°C to 200°C still with a rate of 10°C/min to determine the melting point. The scanning is done under nitrogen atmosphere.

Gel permeation chromatography (GPC) was used to determine the molecular weight averages and distribution of the polymer. The samples were dissolved in trichlorobenzene and filtered to remove, when present, the insoluble fraction. The remaining solution was then passed through a PL Gel 5 mL Mixed-A column of the chromatograph at 140°C.

The samples are all extracted in xylene to determine the gel content (cross-linked portion). A weighted amount of the sample, $m_1 \approx 1$ g, was put into a soxtex thimble and extracted in ± 35 mL boiling xylene in the soxtex™ 2043 apparatus. After extraction for 6 hours (4 hours boiling and 2 hours rinsing) the soxtex thimbles were removed from the soxtex and dried in an oven at 50°C to a constant weight ($m_2$). This weight corresponds to the insoluble (cross-linked) portion of the sample. The amount of cross-linked iPP was then determined from the relation

$$cross-linked\ iPP\ \ wt\% \ = \frac{m_2}{m_1} \cdot 100\% \qquad (3.1)$$

### 3.3.4 Dynamic shear measurements

The dynamic shear measurements were performed by a RMS 800 apparatus from Rheometric Scientific. This is a controlled shear rate rheometer, which uses two parallel plates with a diameter of 25 mm and a variable gab. The samples were cut from pressed plates. The granules were pressed to plates at 170°C, close to the melting temperature to avoid air bubbles, for 10 minutes. After 10 minutes the plates were removed and cooled down.

First a dynamic sweep strain measurement was performed at 170°C to determine the linear viscoelastic region and the thereby corresponding applied strain. To be in the viscoelastic region of the samples, the strain varied from 4-220%. Then a temperature/frequency sweep measurement was carried out in a temperature region of 170-230°C and in a frequency range from 0.1-100 rad/s.

[4] Calculations can be found in appendix B

### 3.3.5 Extension viscosity measurements

The extensional viscosity was measured with the RME apparatus from Rheometric Scientific. This is a controlled strain rate rheometer. The measurements are performed with rectangular strips of $60 \cdot 7 \cdot 1{,}5\ mm$. These strips were cut from pressed plates. The granules were pressed to plates at 170°C, close to the melting temperature to avoid air bubbles, for 10 minutes. After 10 minutes the plates were removed and cooled down.

The strips were placed in the heat chamber (170°C) of the RME apparatus and placed between two clamps surrounded by toothed belts (figure 8). The clamps rotated in opposite direction at a constant elongation rate of 0.1 $s^{-1}$. The actual strain rate is less than the nominal strain rate that is entered in the RME control program. This is due to some slip at the end of the belts and because the flow profile is never completely uniform. Therefore the stretching of the samples was recorded, so one can determine the formation during the stretching process. The strain rate can then be calculated and the average of the two strain rate is referred to as the true strain rate.

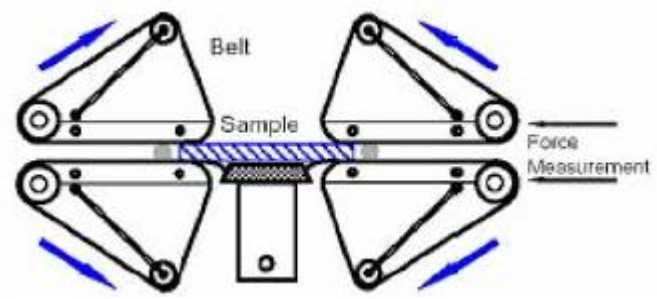


Figure 8: Schematic drawing of RME apparatus[5]

## 3.4 Results and discussion

Each co-agent is used to prepare a set of samples whereby the amount of co-agent is adapted. The set of samples are discussed below and arranged according to the used co-agent. Afterwards, the co-agents are compared with each other. There are no results of the extensional viscosity measurements, since the viscosity of the samples was too low to obtain a homogeneous distribution during the measurements.

*Hydroquinone (HQ)*

The mixing torque is measured during the modification in the melt. A remarkable increase in mixing torque is obtained after the addition of the peroxide, around $t = 360\ s$ (figure 33 Appendix C). Further analysis showed that the higher the amount of HQ, the longer it takes before the mixing torque increases and eventually the increase in mixing torque completely disappears. This indicates that there is an induction time before any reaction occurs, and this induction time appears to correlate with the amount of HQ that is used. After a given time the mixing torque starts to decrease again. This general trend of mixing torque is in consistency with the findings of Romani et al. [24]. However, they did not

[5] http://cdn.grin.com/images/preview-object/document.58506/a1ada51dcc4ec2d3878854763afe6069_LARGE.png

find an induction time. The induction time can be explained with the reaction mechanism of HQ (figure 9). Hydroquinone is a well-known inhibitor which is capable of "consuming" two radicals (figure 7) [43] and is first converted into *p*-benzoquinone before it can react with the free macro-radicals on the iPP chain (figure 9) to eventually form the desired branched structure. The higher amount of HQ can result in a longer conversion time towards *p*-benzoquinone and therefore a longer induction time, however, more research is necessary to verify this hypothesis. When the amount of HQ becomes too high, it is expected that all the radicals are terminated before branching can take place.

The growth of the torque value is caused by the increment of the viscosity, due to the formation of bonds between chains. The decrease of the mixing torque is due to the dispersion of the branched/cross-linked fractions in the not branched/cross-linked matrix [24].

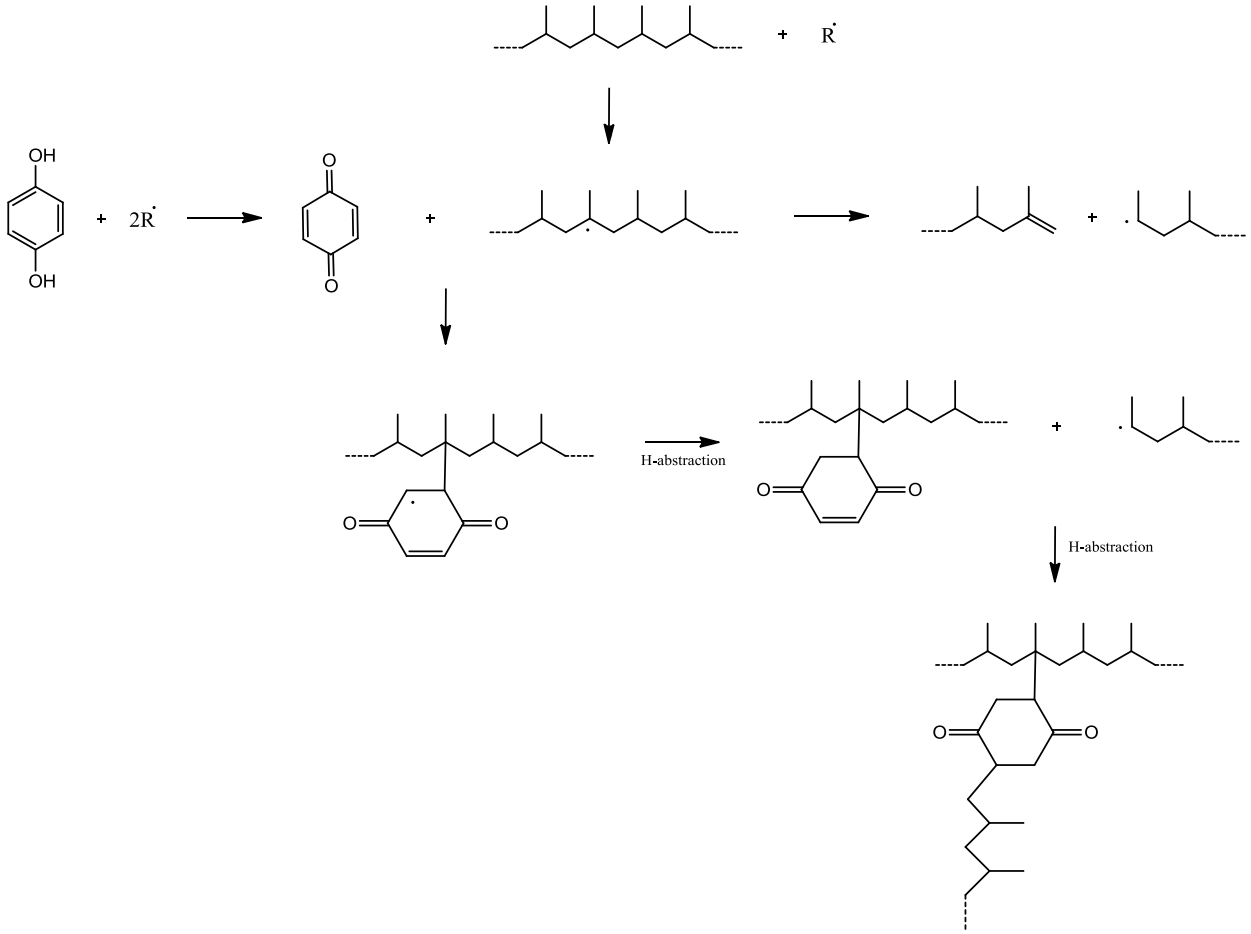


Figure 9: Reaction mechanism with co-agent hydroquinone (based on [43] [45])

After modification with hydroquinone, an increase in crystallization temperature is obtained. After a given amount (>0.4 wt%) of added hydroquinone the crystallization temperature declines again (figure 10). This corresponds with the mixing torque behavior of HQ, where the amount of HQ appears to have effect on the induction time and increase in mixing torque.

This increase in crystallization temperature has also been reported in literature [46] [47] [48]. During the melt modification, degradation, recombination and grafting reactions take place simultaneously. These reactions result in changes of the following molecular factors [6]:

- Molecular weight and its distribution
- Chain irregularity due to branching/crosslinking, grafting of the co-agent, and/or binding of peroxide radicals to the polymer chain

These changes can affect the thermal behavior of the polymer. The formation of long chain branches results in more nucleation points, it is therefore possible to obtain an increase in crystallization temperature. However, an increase in crystallization temperature can also occur when polypropylene degrades, because degradation leads to more, smaller, chains. These smaller chains act as nucleating points and are capable in raising the crystallization temperature. To enclose this effect, the starting $T_c$ (HQ = 0 wt%) is from the thermally treated sample (degraded iPP).

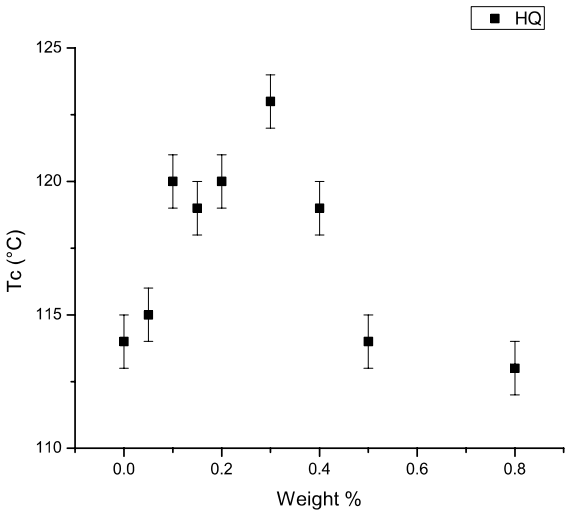


Figure 10: Crystallization temperature vs. weight fraction HQ

More insight about the formed structure can be obtained by the molecular weight and the gel content (table 2). On the basis of the purposes and the reaction mechanism (figure 9), it is sufficient to say that an increase in the molecular weight average, in comparison to the reference sample #5, together with an increase in crystallization temperature and no (or low) gel content, indicates the formation of long chain branches. However, since the calibration of the GPC apparatus is performed with polystyrene, the average molecular weight cannot be used as an absolute value but only to show trends.

The mixing torque, crystallization temperature, the trend of $M_w$ average and the zero gel content, indicates that the samples #18, #19, #20, #21 and #53 have a branched structure. To verify the existence of branches shear rheology measurements were performed (figures 11 and 12).

| Sample # | Co-agent | Amount of co-agent (wt%) | Gel content (%) | $M_w$ | $M_w/M_n$ |
|---|---|---|---|---|---|
| **5** | - | - | - | 81069 | 6.2 |
| **18** | HQ | 0.1 | 0 | 134648 | 5.7 |
| **19** | HQ | 0.15 | 0 | 145689 | 6.6 |
| **20** | HQ | 0.2 | 0 | 190658 | 6.5 |
| **21** | HQ | 0.3 | 0 | 127540 | 5.7 |
| **53** | HQ | 0.4 | 0 | n.a. | n.a. |
| **45** | HQ | 0.5 | 0 | 137197 | 6.5 |
| **43** | HQ | 0.8 | 0 | 125976 | 5.6 |

Table 2: List of samples modified with HQ

The storage modulus, $G'\ \omega$ , of all the modified samples is significantly higher at low frequency when compared to the thermally treated sample #5 (figure 11), taken here as reference material. The modified samples show a decrease in the slope of $G'\ \omega$ suggesting non-terminal behavior which implies a longer relaxation mechanism, hinting to the possible creation of some long chain branches formed in the melt.

Another way to investigate the presence of LCB involves the examination of the loss angle $\delta$ [4] which is plotted versus the frequency. The figure shows an increase in elasticity (decrease in loss angle) when HQ is added, until a certain point (#53 0.4 wt%) when the elasticity declines again (figure 12). This behavior was already expected, due to the consumption of radicals by HQ (figure 7), the results found for the crystallization temperature and the behavior of the mixing torque.

According to literature, linear iPP should display a monotonically decreasing curve of $\delta\ \omega$ , while for branched samples the curve changes in position and in form [37].

An increase in elasticity can be obtained due to long chain branches as well as a higher average molecular weight or the broadening of the molecular weight distribution. However, the molecular weight distribution is in the same range for all the samples (table 2). The results (figure 12) are shifted at 170°C (time-temperature superposition) and the samples #18, #20, #21 and #53 show dispersion while the modified samples #45 and #43 show excellent superposition. Dispersion is typical behavior for a branched (or cross-linked) structure, while superposition is typical behavior for linear polymers [42].

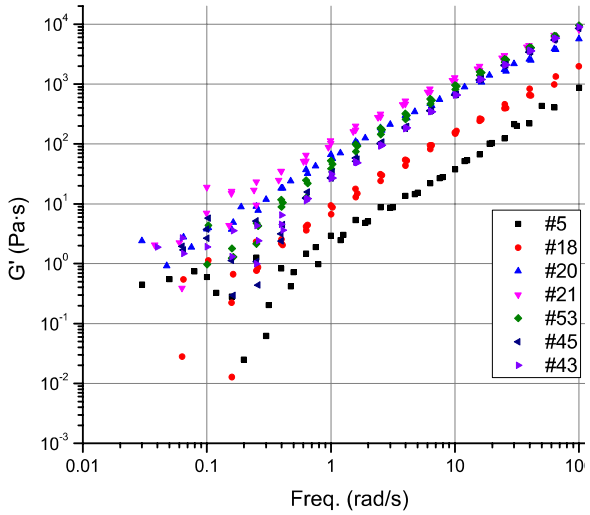


Figure 11: Storage modulus vs. frequency for the linear iPP and the samples modified with HQ (shifted at 170C°)

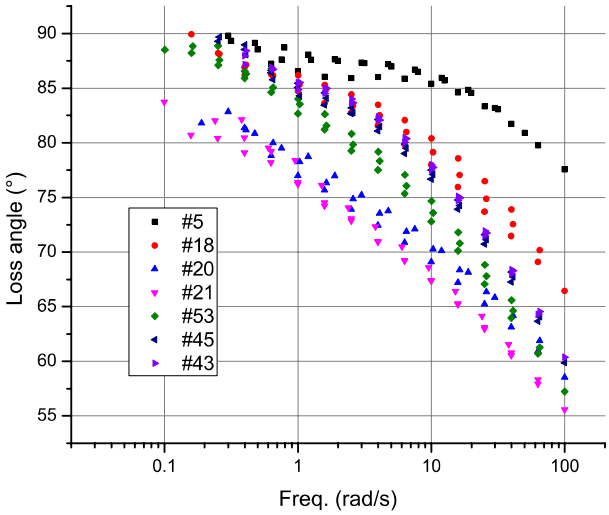


Figure 12: Loss angle vs. frequency (shifted at 170°C) for iPP melts modified with HQ

All the modified samples show an increase in zero shear viscosity (figure13). The increase in $\eta^* \ \omega \to 0$ can indicate the formation of branches, but can also be obtained due to a higher molecular weight. The samples #18, #20, #21 and #53 display shear thinning behavior at lower shear rates then the samples #5, #45 and #43. The addition of branches or the broadening of the molecular weight distribution results in a more compact polymer chain and therefore the polymer behaves as a non-Newtonian fluid at lower shear rates [34]. Based on this theory, it is expected that the higher zero shear rate of sample #45 and #43, is created by a higher average molecular weight instead of the introduction of branches.

On the other hand, the rheological behavior in combination with the absence of any gel amount, the mixing torque behavior and the $T_c$, leads to the conclusion that the samples #18, #20, #21 and #53 have a slightly branched structure. The decrease of branching seems to increase with the amount of HQ present. The only sample that deviates from this trend is #53 with 0.4 wt% HQ. It seems that there is an optimum in the amount of co-agent and any amount above this has an adverse effect on the probability of branches. Borsig et al. [4] also suggested that there could be an optimum for the amount of co-agent and the probability of branches.

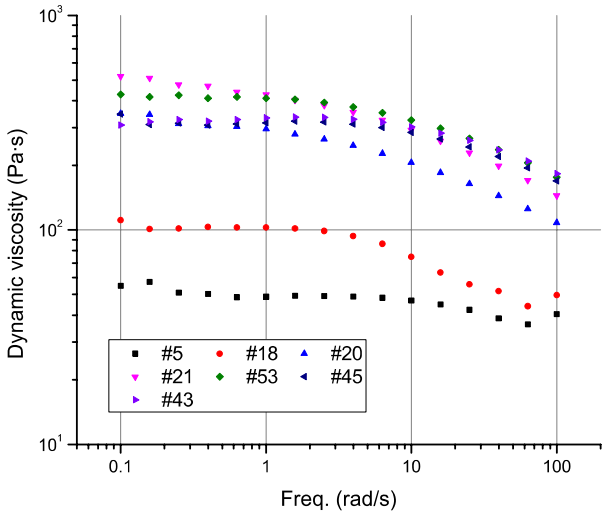


Figure 13: Viscosity vs. frequency for iPP melts modified with HQ

*p-Benzoquinone (BQ)*

The plastogram (figure 34 Appendix C) shows an increase in mixing torque after the addition of the peroxide and after a certain point the mixing torque decreases again. As discussed before, the increase is caused by the formation of a branched/cross-linked structure and the decrease due to the dispersion of the branched/cross-linked fraction in the not branched/cross-linked matrix.

The DSC measurements show an increase in crystallization temperature after modification with BQ (figure 14). The increase in crystallization temperature can be an indication for some branching. In combination with the measured gel content of these samples (table 3), the conclusion can be drawn that the increase in crystallization temperature of the samples #55, #52 and #41 is obtained due to a cross-linked structure.

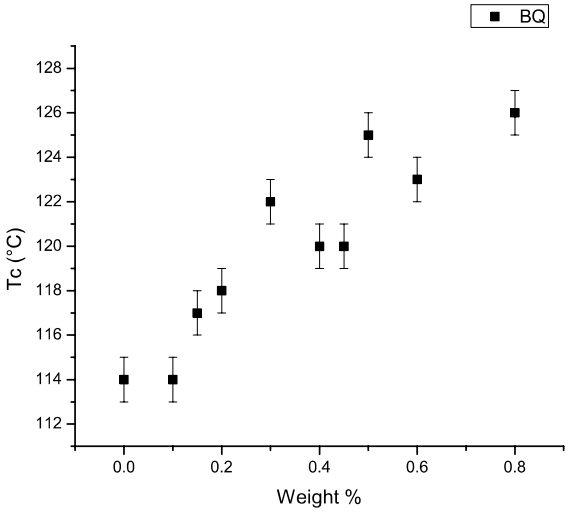


Figure 14: Crystallization temperature vs. weight fraction BQ

| Sample # | Co-agent | Amount of co-agent (wt%) | Gel content (%) | $M_w$ | $M_w/M_n$ |
|---|---|---|---|---|---|
| **5** | - | - | 0 | 81069 | 6.2 |
| **32** | BQ | 0.1 | 0 | 110235 | 6.0 |
| **34** | BQ | 0.2 | 0 | 122997 | 6.1 |
| **35** | BQ | 0.3 | 0 | 125482 | 5.3 |
| **36** | BQ | 0.4 | 0 | 108935 | 6.4 |
| **55** | BQ | 0.5 | 58.2 | n.a. | n.a. |
| **52** | BQ | 0.6 | 7.4 | n.a. | n.a. |
| **41** | BQ | 0.8 | 16.8 | n.a. | n.a. |

Table 3: List of samples modified with BQ

A better indication for the formation of LCB is given by the rheology measurements. The storage modulus, $G'\ \omega$ , is significantly higher for the samples modified with BQ then for the thermally treated linear sample #5 (figure 15). The absolute value of the elastic moduli seems to increase with the amount of BQ present, but at a given intake (0.4 wt%) the moduli starts to decrease again. This indicates that there is an optimum in the amount of co-agent and any amount above this has an adverse effect on the probability of branches. This trend was also observed when HQ was used as co-agent. The storage modulus of sample #55 is much higher than the storage modulus of the other samples, the high elastic response of this sample is created by the highly cross-linked structure (table 3).

The plot of the loss angle versus the frequency can give a good indication for the presence of branches. The plot is shifted at 170°C (time-temperature superposition) and the samples #34, #35, #36 and #55 show dispersion (figure 16). As discussed before, linear polymers exhibit excellent superposition while a branched structure results in dispersion.

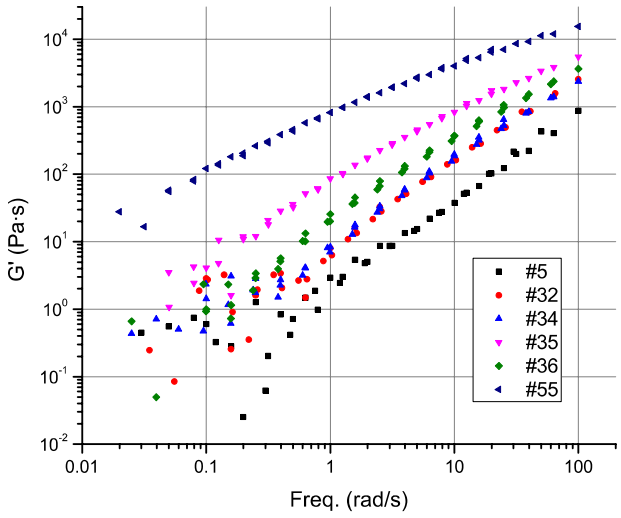


Figure 15: Storage modulus vs. frequency for the linear iPP and the samples modified with BQ (shifted at 170C°)

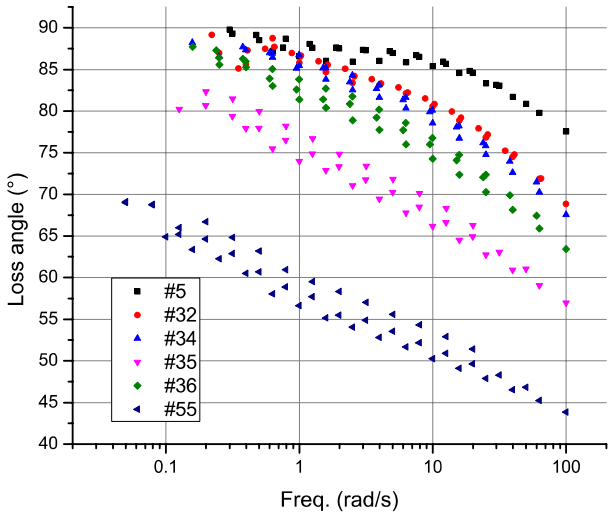


Figure 16: Loss angle vs. frequency (shifted at 170°C) for iPP melts modified with BQ

These findings are in consistency with the viscosity measurements, where an increase in $\eta^*$ can be observed for the samples modified with BQ (figure 17). The rheological behavior in combination with the absence of any gel amount, the mixing torque behavior and the increase in $T_c$, leads to the conclusion

that the samples #34, #35 and #36 have a slightly branched structure. Furthermore, the elastic properties of sample #55 are derived from the highly cross-linked structure.

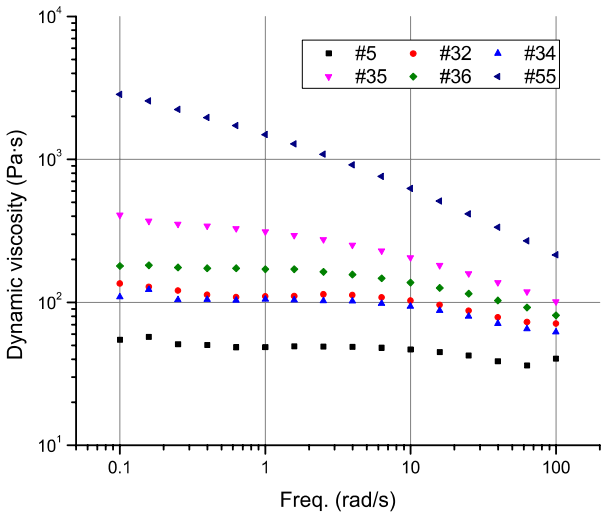


Figure 17: Viscosity vs. frequency for iPP melts modified with BQ

*Methyl-p-benzoquinone (MBQ)*

Methyl-p-benzoquinone is a co-agent with two double bonds that differ in reactivity. One "highly" reactive double bond to quickly stabilize the macro-radicals, and one lower reactive double bond which eventually reacts to form the desired branched structure. The reaction is shown by the increase in mixing torque after the addition of the peroxide (figure 35 Appendix C). The increase is mixing torque is obtained when ≥ 0.2 wt% MBQ is added. From that moment on, there seems to be an induction time which increases when the amount of MBQ increases. An explanation for this might be found in the reaction mechanism (figure 18). First the highly reactive double bond stabilizes the macro-radicals, this reaction does not cause an increase in mixing torque. After a certain point, when (most of) the co-agent is grafted on the macro-radicals, the less reactive double bond starts to react with secondary radicals to form LCB-iPP which causes the increase in mixing torque. To verify this hypothesis, more research needs to be performed.

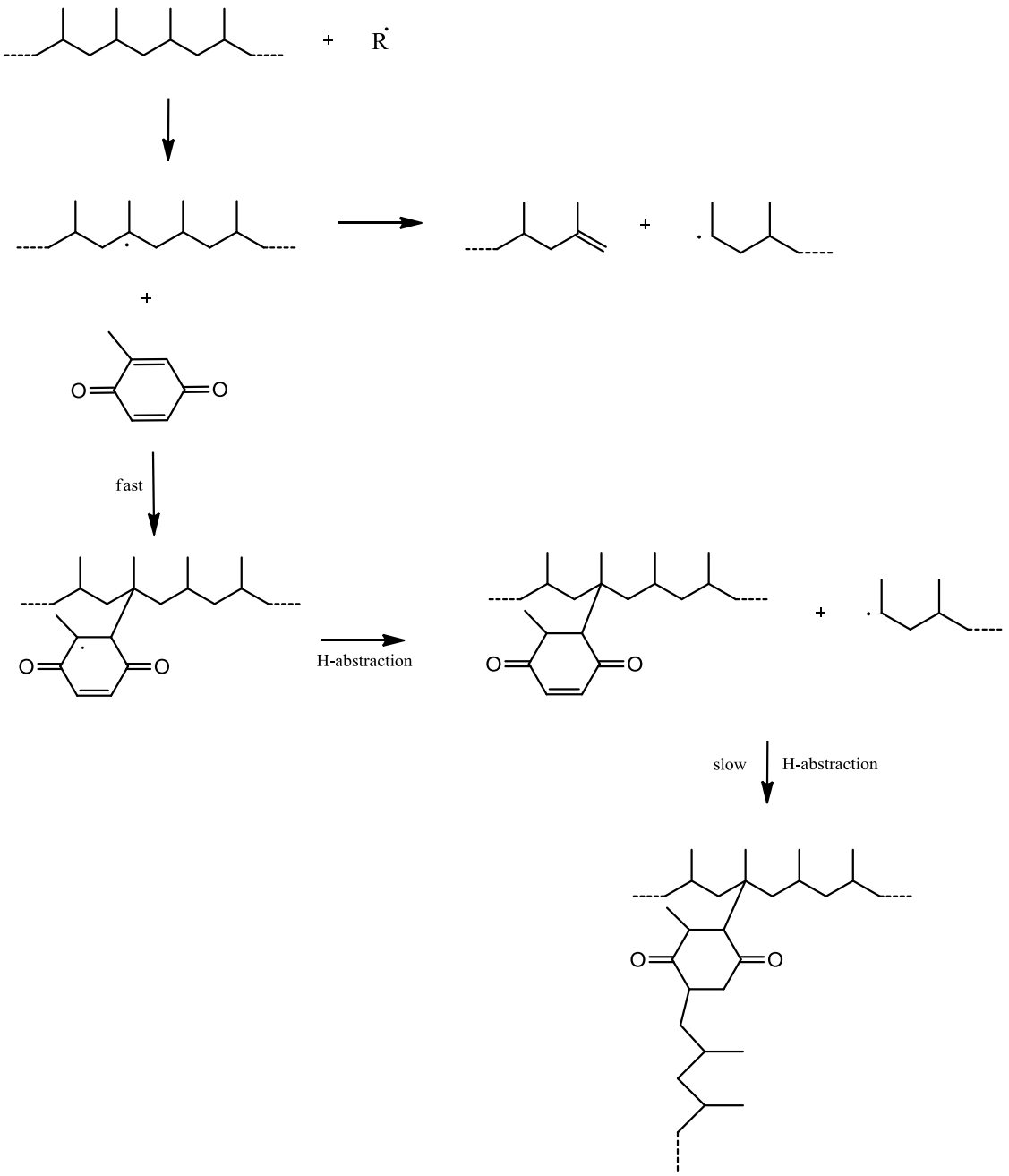


Figure 18: Reaction mechanism with co-agent methyl-p-benzoquinone

An increase in crystallization temperature is obtained when ≥0.2 wt% MBQ is added (figure 19). This corresponds with the start of the increase in mixing torque. Furthermore, an increase in average molecular weight is obtained without formation of any amount of gel (table 4), thus strongly suggesting the formation of LCB when ≥0.2 wt% MBQ is used.

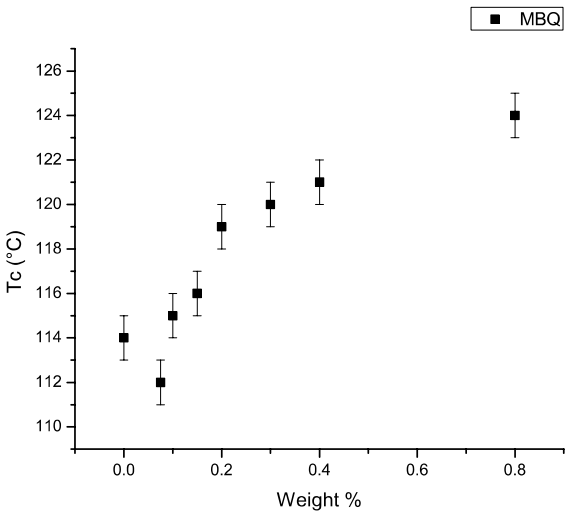


Figure 19: Crystallization temperature vs. weight fraction MBQ

| Sample # | Co-agent | Amount of co-agent (wt%) | Gel content (%) | $M_w$ | $M_w/M_n$ |
|---|---|---|---|---|---|
| **5** | - | - | 0 | 81069 | 6.2 |
| **51** | MBQ | 0.075 | 0 | 105521 | 5.8 |
| **44** | MBQ | 0.1 | 0 | 92317 | 5.4 |
| **46** | MBQ | 0.15 | 0 | 94461 | 6.6 |
| **47** | MBQ | 0.2 | 0 | 112720 | 6.3 |
| **58** | MBQ | 0.3 | 0 | 129886 | 6.3 |
| **56** | MBQ | 0.4 | 0 | 111101 | 6.4 |
| **57** | MBQ | 0.8 | 0 | 111391 | 6.0 |

Table 4: List of samples modified with MBQ

These preliminary conclusions need to be confirmed with rheology measurements, which gives more information on the molecular structure of the modified samples. The $G'\ \omega$ curve of the modified samples closely resembles the one for the references iPP (figure 20). Only a minor increase of the storage modulus is obtained when MBQ is used as co-agent. At high amounts of MBQ (0.8 wt%) the slope of $G'\ \omega$ decreases and the absolute value increases. When the loss angle is plotted against the frequency and shifted at 170°C, the samples #47, #44, #58 and #56 show some dispersion (figure 21), hinting to the possible creation of some long branches. However, the high value of the loss angle indicates that the destructive effect of the peroxide prevails. Only at high amounts of MBQ the elasticity really increases (sample #57).

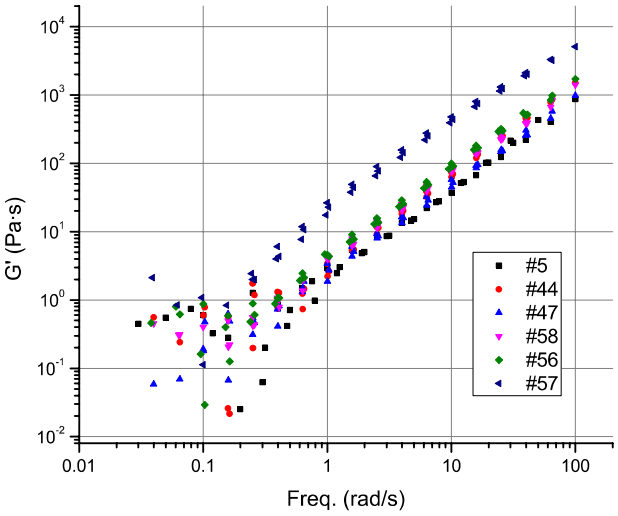


Figure 20: Storage modulus vs. frequency for the linear iPP and the samples modified with MBQ (shifted at 170C°)

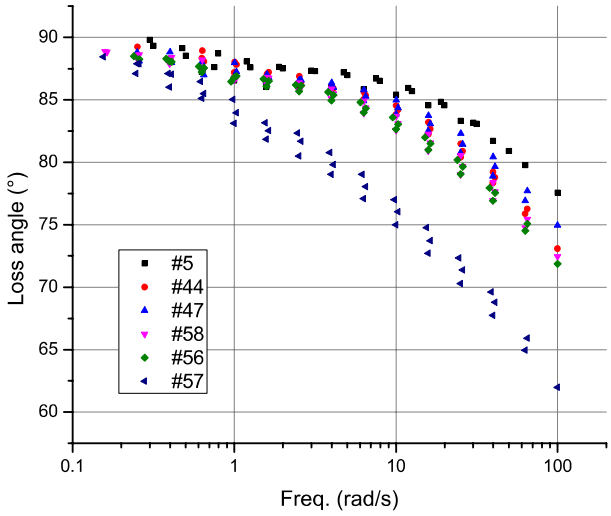


Figure 21: Loss angle vs. frequency (shifted at 170°C) for iPP melts modified with MBQ

All the samples modified with MBQ show higher values for the dynamic viscosity then the reference sample #5 (figure 22), but they only show a slight increase. The dynamic viscosity increases with the amount of co-agent used. The only sample that deviates from this trend is sample #47. It is not clear why sample #47 deviates from this trend. It can be possible that the reaction has not been carried out successfully, but to verify this, more research needs to be performed.

The mixing torque behavior, increase in crystallization temperature and the increase in molecular weight hint to the formation of long chain branches. As a result, it is expected that the minor increase in elasticity (figure 21) is caused by the formation of some long branches. However, the degradation reaction seems to prevail. At higher levels of MBQ, the formation of long chain branches starts to prevail and an increase in elasticity is obtained (sample #57).

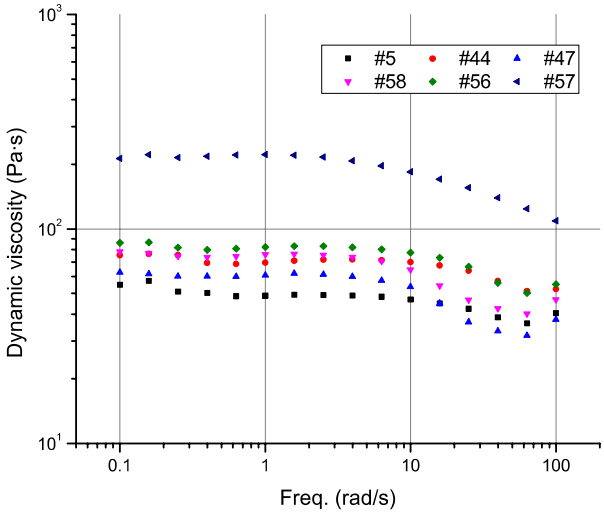


Figure 22: Viscosity vs. frequency for iPP melts modified with MBQ

*Divinylbenzene (DVB)*

The mixing torque increases after the addition of the peroxide (figure 36 Appendix C). The increase in mixing torque becomes bigger with the quantity of DVB used. But then it decreases rather quickly in comparison with the mixing torque behavior when HQ, BQ or MBQ is used as a co-agent. This indicates that the consumption of the co-agent happens fast and that afterwards the only proceeding reaction is degradation. This behavior was also observed by Zhang et al. [20] when DVB was used as co-agent and by Romani et al. [24] when a bis maleimide co-agent was used.

An increase in crystallization temperature is obtained when 0.2 wt% DVB or more is added (figure 23). A large increase in average molecular weight is obtained when DVB is used as co-agent and according to the gel content; a cross-linked structure is only obtained when high amounts of DVB are used (table 5).

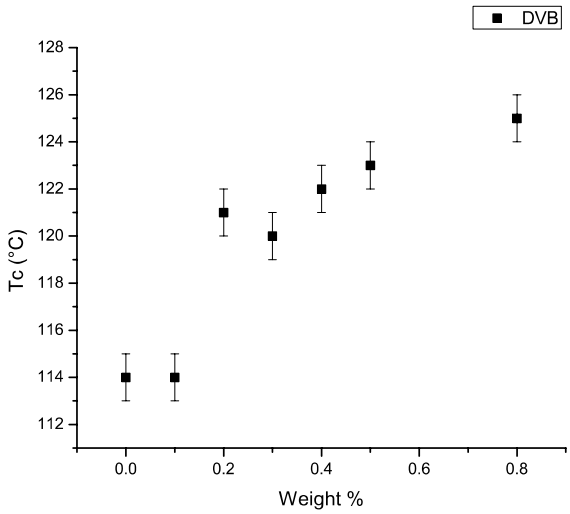


Figure 23: Crystallization temperature vs. weight fraction DVB

| Sample # | Co-agent | Amount of co-agent (wt%) | Gel content (%) | $M_w$ | $M_w/M_n$ |
|---|---|---|---|---|---|
| **5** | - | - | 0 | 81069 | 6.2 |
| **6** | DVB | 0.1 | 0 | 211241 | 7.1 |
| **7** | DVB | 0.2 | 0 | 197754 | 7.0 |
| **8** | DVB | 0.3 | 0 | 190234 | 8.5 |
| **59** | DVB | 0.4 | 0 | 146977 | 6.2 |
| **60** | DVB | 0.5 | 0 | 199582 | 6.8 |
| **61** | DVB | 0.8 | 25.9 | 197766 | 7.3 |

Table 5: List of samples modified with DVB

For the samples #7 and #8 the shape of the $G'\ \omega$ curves remains the same as those of the thermally treated linear iPP (sample #5) and no significant increase of the moduli is obtained (figure 24). They exhibit the typical terminal flow behavior, indicating that they are linear. Sample #6 even shows an

increase in the slope of $G'\ \omega$ (terminal flow behavior). However, sample #59, #60 and #61 show a decrease in the slope of $G'\ \omega$ hinting to the possible formation of branches.

The elasticity of the samples seems to increase with increasing amount of DVB (figure 25). This can be due to introduction of long chain branches, as well as due to a higher average molecular weight or due to broadening of the molecular weight distribution.

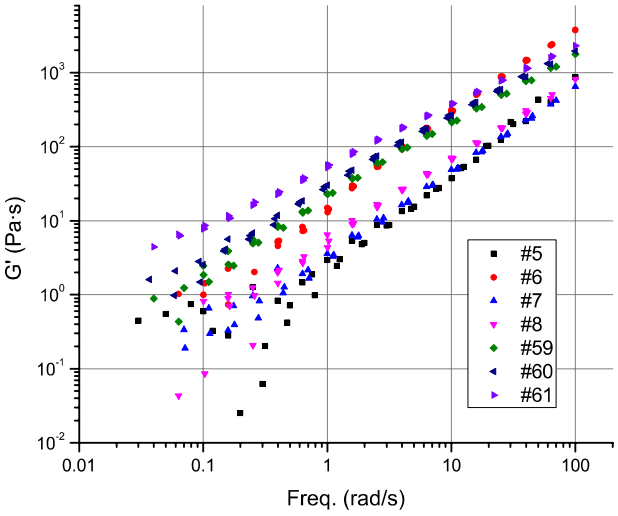


Figure 24: Storage modulus vs. frequency for the linear iPP and the samples modified with DVB (shifted at 170C°)

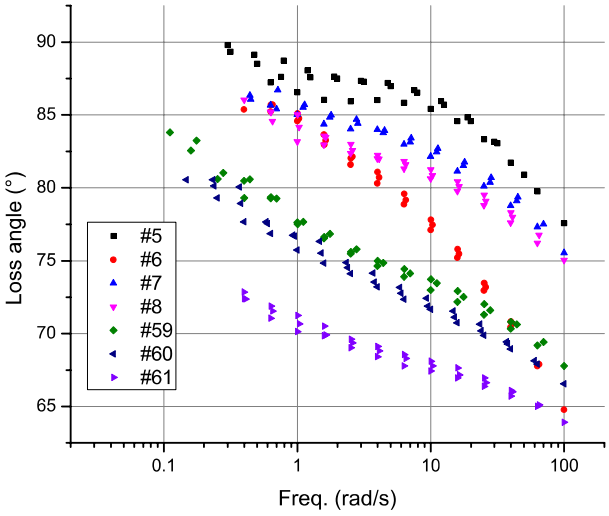


Figure 25: Loss angle vs. frequency (shifted at 170°C) for iPP melts modified with DVB

The samples #7 and #8 show no increase in viscosity (figure 26) which is not in consistency with the GPC data (table 5). An increase in molecular weight should give an increase in $\eta^*\ \omega \to 0$ according to the following relation:

$$\eta_0 = K\ Mw_{av}{}^{3.4}$$

which was described in chapter 2, section 2.3.2. According to this relation, the increase in viscosity should be higher for all the modified samples when compared to the reference sample #5. Therefore, the GPC data need to be interpreted with caution.

The samples #59, #60 and #61 behave non-Newtonian at lower shear rates. The addition of branches or the broadening of the molecular weight distribution results in a more compact chain and therefore non-Newtonian behavior at lower shear rates [34]. In combination with the gel content found for sample #61, the behavior of sample #61 is caused by a cross-linked structure. While the lower slope of the $G'\ \omega$ curve and the decrease in loss angle of the samples #59 and #60, together with the zero gel content and increase in crystallization temperature indicates a slightly branched structure.

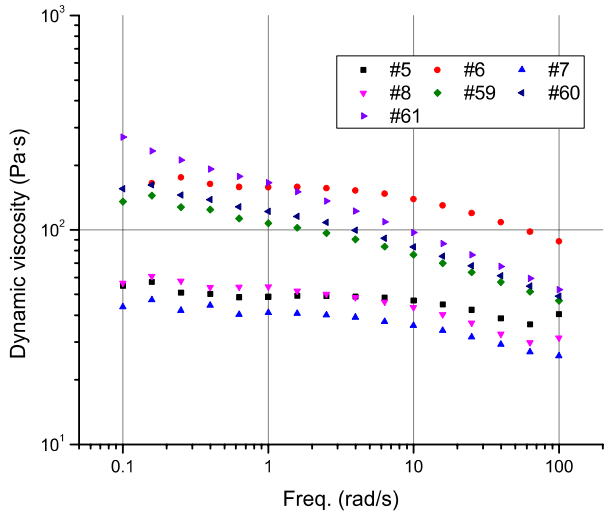


Figure 26: Viscosity vs. frequency for iPP melts modified with DVB

The results show that at low levels of DVB, the degradation reaction prevails resulting in a high loss angle (viscous material). While at higher levels of DVB, the crosslinking reaction prevails, this can be seen by the decrease in loss angle and the lower slope of the $G'\ \omega$ curve. This behavior was also observed by Borsig et al. [4] and is expected to be caused by the self-polymerisable ability of DVB.

*Allyl-2-furoate (A2F)*

Allyl-2-furoate has two different kinds of carbon-carbon double bonds and is a self-polymerisable monomer. This can result in the preferred branching reaction or it becomes highly susceptible towards crosslinking and/or homo-polymerization (figure 27).

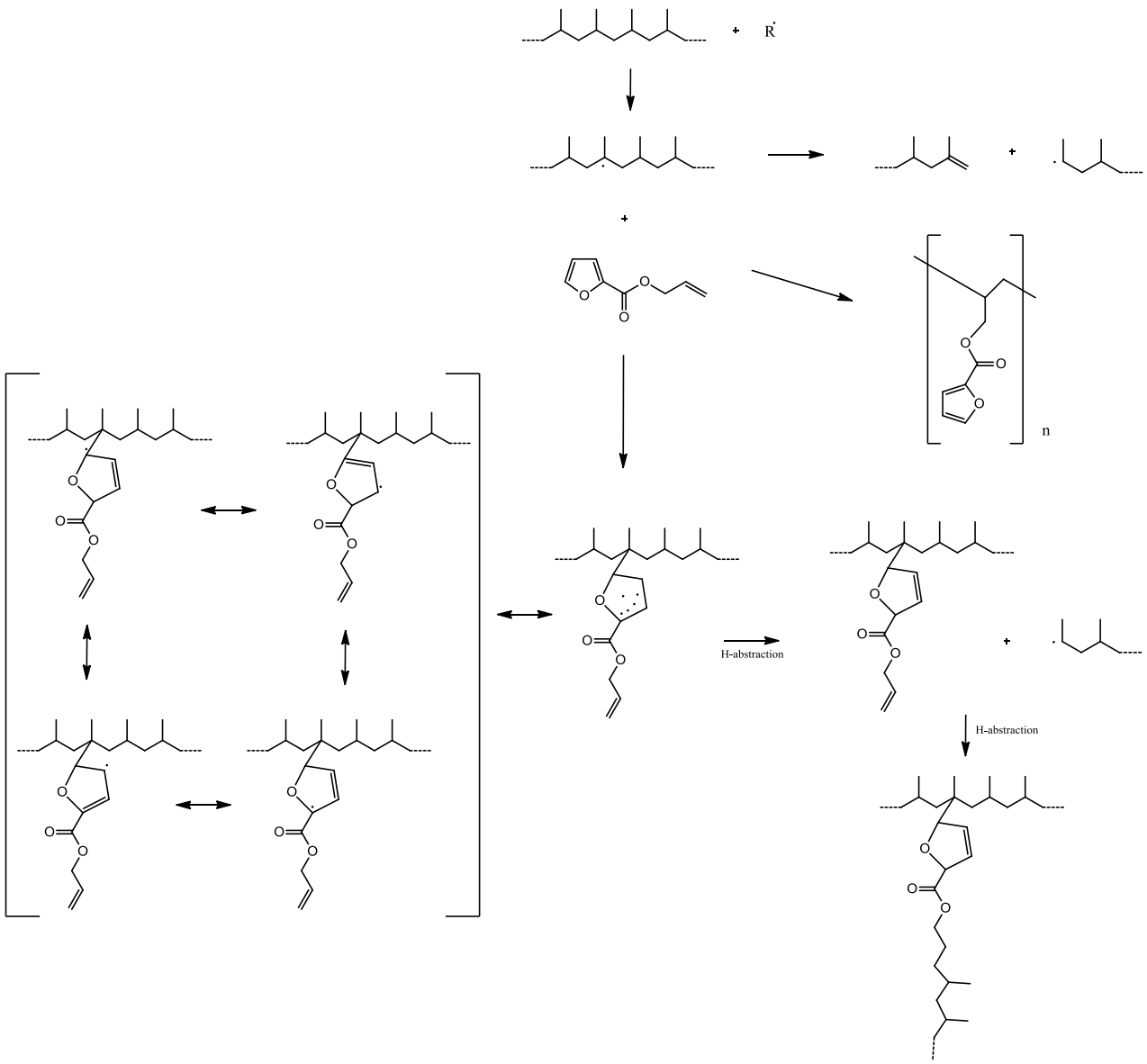


Figure 27: Reaction mechanism with co-agent allyl-2-furoate

When A2F is used as co-agent, no increase in mixing torque is obtained after the addition of the peroxide (figure 37 Appendix C). The mixing torque remains decreasing after the addition of the peroxide. As described earlier, when a branched or cross-linked structure is formed an increase in mixing torque is obtained. It is therefore expected that A2F is not capable in inducing a branched structure. Other indications for this hypothesis are the crystallization temperature (figure 28) and the GPC data (table 6) which remains approximately the same as for the reference experiment. A possible explanation for this can be the self-polymerisable ability of the co-agent [44], which can result in homo-polymerization instead of branching (figure 27).

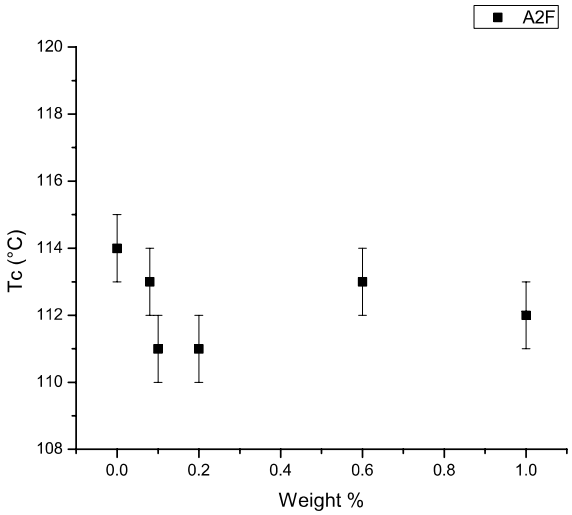


Figure 28: Crystallization temperature vs. weight fraction A2F

| Sample # | Co-agent | Amount of co-agent (wt%) | Gel content (%) | $M_w$ | $M_w/M_n$ |
|---|---|---|---|---|---|
| **5** | - | - | 0 | 81069 | 6.2 |
| **66** | A2F | 0.075 | 0 | 79434 | 5.8 |
| **63** | A2F | 0.1 | 0 | 90426 | 5.9 |
| **64** | A2F | 0.2 | 0 | 74068 | 5.8 |
| **65** | A2F | 0.6 | 0 | 77311 | 6.0 |
| **67** | A2F | 1 | 0 | 85152 | 6.4 |

Table 6: List of samples modified with A2F

When A2F is used as co-agent, the shape of the $G'$ $\omega$ curves remains the same and the moduli is slightly lower than those of the blank experiment (figure 29). An increase in loss angle is observed as well (figure 30), indicating that the degradation reaction prevails.

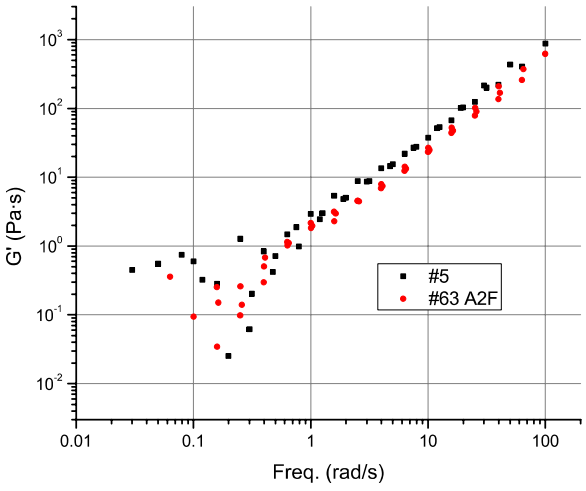


Figure 29: Storage modulus vs. frequency for the linear iPP and the samples modified with A2F (shifted at 170C°)

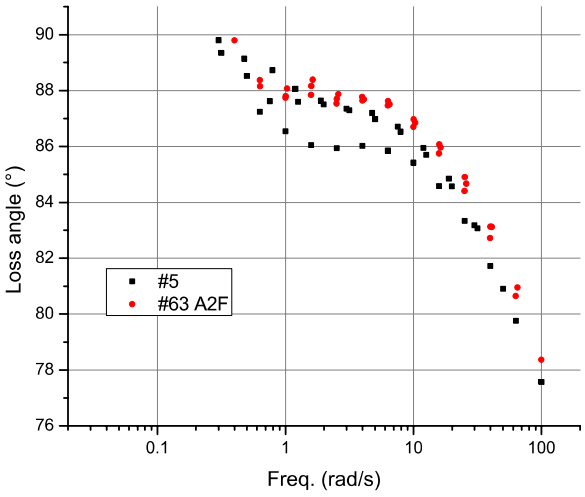


Figure 30: Loss angle vs. frequency (shifted at 170°C) for iPP melts modified with A2F

The decrease in dynamic viscosity is caused by degradation (figure 31). The shear rheology measurements verify that no branches were produced when A2F is used as co-agent. It is expected that homo-polymerization of A2F prevails. A possible explanation for this can be found in the solubility of A2F in iPP. A2F is not highly soluble in iPP which can result in poor dispersion of A2F, making it even more susceptible for homo-polymerization.

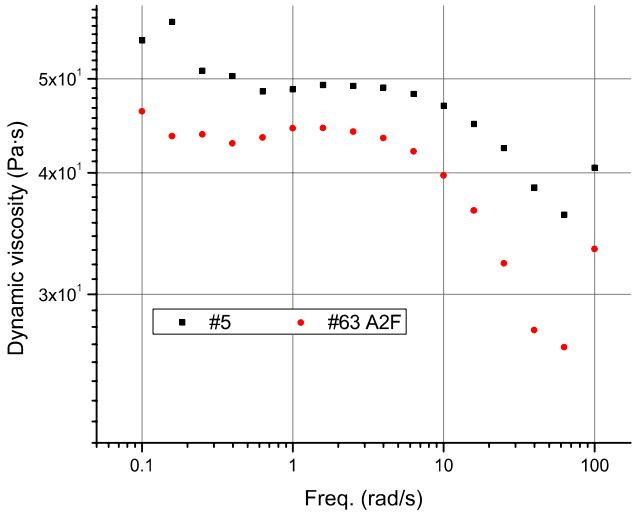


Figure 31: Viscosity vs. frequency for iPP melts modified with A2F

*Comparison of the co-agents*

It should be obvious from the above results that A2F is not considered in this section, since A2F is not capable in producing the branched structure. An attempt was made to correlate the co-agent (HQ, BQ, MBQ and DVB) properties with the zero shear viscosity, but it was not possible to fit the data in a statistically significant way.

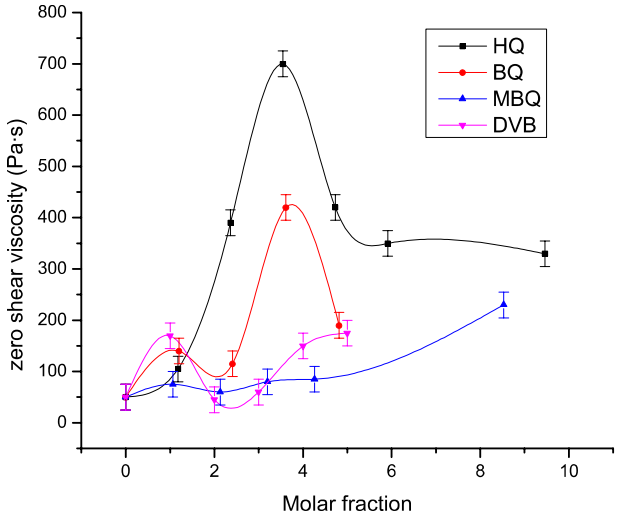


Figure 32: Zero shear viscosity vs. molar fraction

To compare the different co-agents, the zero shear viscosity is plotted against the molar fraction (figure 32), the samples that had a gel content are not displayed in the figure. It is expected that the difference in efficiency of the co-agents can be understood from their difference in solubility, their different reactivity's and the reaction mechanism.

When the co-agents are ranked on basis of their compatibility with iPP (table 1), the ranking is as follows:

$$DVB > A2F > MBQ > BQ > HQ$$

However, the zero shear viscosity of the samples shows a completely different ranking (figure 32). The success of the branching of iPP seems to be independent of the solubility of the co-agent in iPP. Of course some solubility of the co-agent in iPP is necessary to ensure dispersion. But, according to these results, it can be stated that the success of branching depends primarily on the reactivity and reaction mechanism of the co-agent.

HQ and BQ display the same trend; they first show an increase in $\eta_0$ and after a certain amount of co-agent the $\eta_0$ declines again. There seems to be an optimum in the amount of co-agent and any amount above this has an adverse effect on the probability of branches. This trend was also observed by Borsig et al. [4] and discussed earlier in this chapter.

The pronounced reaction mechanism of HQ shows that HQ first acts as stabilizer and is converted to BQ (figure 9), this means that the mixture changes continuously. In the beginning the amount of usable co-agent (BQ) is zero and during the modification more BQ is produced and the radicals are consumed by the conversion of HQ towards BQ.

The zero shear viscosity of HQ lies significant higher than the zero shear viscosity of BQ. The only difference in reaction mechanism and reactivity between HQ and BQ is the conversion of HQ towards BQ which results in an induction time. It can therefore be stated that the induction time has a positive influence on the resulting structure.

For branching to occur, secondary radicals are necessary to react with the grafted co-agent. During the induction time, β-scission of the iPP chains can take place and secondary radicals are formed which can afterwards react with the grafted co-agent to form the branched structure.

Furthermore, according to Parent et al. [14] [15], the grafting co-agent is preferentially grafted to high molecular weight chains, the grafting of a co-agent makes the chain more reactive with respect to molecular weight growth and therefore has a heightened capacity for crosslinking. Therefore a high amount of co-agent will result in crosslinking; this is exactly what is observed when BQ is used as co-agent. This effect is not observed when HQ is used; it is expected that when high amounts of HQ are used all the radicals are terminated by the conversion towards BQ.

When the co-agent MBQ is used, the reactivity of the two double bonds is completely different. The higher reactive double bond first grafts onto the iPP chain to form the stable macro-radical and then the lower reactive double bond reacts with a secondary radical to form the branched structure. An increase in zero shear viscosity only occurs when high amounts of MBQ are used (figure 32). It is therefore expected that when low amounts of MBQ are used only the grafting reactions occurs. An explanation for this can be found in the reactivity of the double bonds (table 1), $\Delta e_{\ 1} = 0.074$ and $\Delta e_{\ 2} = 0.005$. Most probably, the second double bond is not reactive enough to promote branching when low amounts of

MBQ are used. MBQ was selected to suppress crosslinking and promote branching. It proved to be effective in suppressing crosslinking when high amounts of co-agents are used, but it is ineffective in promoting branching. The co-agents HQ and BQ proved to be more effective co-agents then MBQ for branching iPP.

DVB is a self-polymerisable monomer, it is quite soluble in iPP and the double bonds can react very easily [4]. Since it is a self-polymerisable monomer, homo-polymerization of DVB can take place as side reaction. This results in an uncontrolled process, where homo-polymerization, branching and crosslinking reactions occur at the same time. The low zero shear viscosity of DVB (figure 32) shows that the use of a self-polymerisable monomer is not suitable to induce LCB, but results in an uncontrolled process. These phenomena were also observed by other researchers [4] [20].

Summarizing the above, the following ranking regarding the ability to produce long chain branches can be obtained:

$HQ > BQ \gg MBQ > DVB \gg A2F$

## 3.5 Conclusions

The present work shows that the choice of co-agent is of enormous importance regarding the ability to induce long chain branches. The most important factors that need to be considered by selecting a co-agent can be summarized as follows:

- A co-agent needs two (or more) double bonds able to react with the formed macro-radicals and at least be bi-functional.
- The use of a polymerisable multifunctional co-agent results in an uncontrolled process where homo-polymerization, branching and crosslinking occur at the same time.
- The solubility of the co-agent in iPP is of less importance as the reactivity and reaction mechanism of the co-agent.
- The reactivity of the double bonds needs to be high enough. When the reactivity is too low, no reaction occurs or it takes a long time before reactions occur. A highly reactive co-agent is preferred.

Other important findings in this work are:

- The introduction of an induction time is preferred to ensure secondary radicals. Secondary radicals are required to induce long chain branches and can be formed through β-scission during the induction time.
- The amount of co-agent and peroxide need to be restricted to avoid crosslinking and degradation.

Furthermore, the following ranking regarding the efficiency to produce long chain branches is obtained:

$HQ > BQ \gg MBQ > DVB \gg A2F$

# 4 Final remarks

Long chain branching on linear polypropylene enhances its strain hardening behavior in elongational flow. Therefore, in contrast to linear iPP, LCB-iPP can be used in processes were elongational flow is dominant. To reach an industrial implementable process, control over the reactions is necessary. In this research, an attempt was made to correlate the co-agent properties with the rheology properties. But it was not possible to fit the data in a statistically significant way. For another attempt, it will be useful to use even more different co-agents.

It was found in this research that an induction time is preferred to induce a branched structure. To ensure this effect more research is necessary. More insight can be gained when a sample is removed every minute and the reaction is quenched. The samples can be extracted with water and acetone to remove the low-molecular weight products and can then be characterized with NMR. This can give a good indication which reactions are taking place. This provides a good method to compare samples with different co-agents and comparing samples with hydroquinone and *p*-benzoquinone can provide more prove for the effectiveness of an induction time.

Furthermore, it will be useful to use another free radical initiator in further research. Due to the half life time of dicumyl peroxide, the working temperature is 170°C. This is very close to the melting temperature of iPP $T_m = 166°C$ . Working in this range results in a more viscous material then when working at a higher temperature. This results in high shear forces in the Brabender and therefore more degradation occurs. To restrain degradation due to shear forces, it is useful to use a free radical initiator that can be used at a temperature around 180°C.

# Bibliography


[1] S. G. Hatzikiriakos, "Long chain branching and polydispersity effects on the rheological properties of polyethylens," *Polymer Engineering and Science,* vol. 40, pp. 2279-2287, 2000.

[2] J. A. Langston, R. H. Colby and T. C. Chung, "Synthesis and characterization of long chain branched isotactic polypropylene via metallocene catalyst and T-reagent," *Macromolecules ,* vol. 40, pp. 2712-2720, 2007.

[3] M. Sugimoto, Y. Suzuki, K. Hyun, K. H. Ahn, T. Ushioda, A. Nishioka, T. Taniguchi and K. Koyama, "Melt rheology of long-chain-branched polypropylenes," *Rheologica Acta,* vol. 46, pp. 33-44, 2006.

[4] E. Borsig, M. van Duin, A. D. Gotsis and F. Picchioni, "Long chain branching on lineair polypropylene by solid state reactions," *European Polymer Journal,* vol. 44, pp. 200-212, 2008.

[5] B. Krause, M. Stephan, S. Volkland, D. Voigt, L. Hausler and H. Dorschner, "Long-chain branching of polypropylene by electron-beam irradiation in the molten state," *Journal of Applied Polymer Science,* vol. 99, pp. 260-265, 2006.

[6] X. Wang, C. Tzoganakis and G. L. Rempel, "Chemical modification of polypropylene with peroxide/pentaerythritol triacrylate by reactive extrusion," *Journal of Applied Polymer Science,* vol. 61, pp. 1395-1404, 1996.

[7] D. Wan, L. Ma, Z. Zhang, H. Xing, L. Wang, Z. Jiang, G. Zhang and T. Tang, "Controlling degradation and branching reactions of polypropylene by different heteroaromatic ring derivatives," *Polymer Degradation and Stability ,* vol. 97, pp. 40-48, 2012.

[8] H. Xing, Z. Jiang, Z. Zhang, J. Qui, Y. Wang, L. Ma and T. Tang, "Effect of leaving group in dithiocarbamates on mediating melt radical reaction during preparing long chain branched polypropylene," *Polymer,* vol. 53, pp. 947-955, 2012.

[9] W. Zhao, G. Wu and Q. Yang, "Controlling the transition of long- and short-chain branching polypropylene," *Polymer-Plastics Technology and Engineering,* vol. 51, pp. 716-723, 2012.

[10] D. Graebling, "Synthesis of branched polypropylene by a reactive extrusion process," *Macromolecules,* vol. 35, pp. 4602-4610, 2002.

[11] J. Tian, W. Yu and C. Zhou, "The preparation and rheology characterization of long chain branching polypropylene," *Polymer,* vol. 47, pp. 7962-7969, 2006.

[12] R. P. Lagendijk, A. H. Hogt, A. Buijtenhuijs and A. D. Gotsis, "Peroxydicarbonate modification of polypropylene and extensional flow properties," *Polymer,* vol. 42, pp. 10035-10043, 2001.

[13] F. Su and H. Huang, "Rheology and melt strength of long chain branching polypropylene prepared by reactive extrusion with various peroxides," *Polymer Engineering and Science,* vol. 50, pp. 342-351, 2010.

[14] J. S. Parent, A. Bodsworth, S. S. Sengupta, M. Kontopoulou, B. I. Chaudhary, D. Poche and S. Cousteaux, "Structure-rheology relationships of long-chain branched polypropylene: Comparitive analysis of acrylic and allylic coagent chemistry," *Polymer,* vol. 50, pp. 85-94, 2009.

[15] J. S. Parent, S. S. Sengupta, M. Kaufman and B. I. Chaudhary, "Coagent-induced transformations of polypropylene microstructure: Evolution of bimodal architectures and cross-linked nano-particles," *Polymer,* vol. 49, pp. 3884-3891, 2008.

[16] F. Su and H. Huang, "Influence of polyfunctional monomer on melt strength and rheology of long-chain branched polypropylene by reactive extrusion," *Journal of Applied Polymer Science,* vol. 116, pp. 2557-2565, 2010.

[17] D. Wan, H. Xing, Z. Zhang, Y. Wang, L. Wang, Y. Wang, Z. Jiang and T. Tang, "Effect of fullerene C60 on the melt grafting reaction between multifunctional monomer and polypropylene," *Journal of Applied Polymer Science,* vol. published online, pp. 1-9, 2012.

[18] G. J. Nam, J. H. Yoo and J. W. Lee, "Effect of long-chain branches of polypropylene on rheological properties and foam-extrusion performance," *Journal of Applied Science,* vol. 96, pp. 1793-1800, 2005.

[19] A. D. Gotsis and B. L. Zeevenhoven, "The effect of long chain branching on the processability of polypropylene in thermoforming," *Polymer Engineering and Science,* vol. 44, pp. 973-982, 2004.

[20] Z. Zhang, D. Wan, H. Xing, Z. Zhang, H. Tan, L. Wang, J. Zheng, Y. An and T. Tang, "A new grafting monomer for synthesizing long chain branched polypropylene through melt radical reaction,"

*Polymer,* vol. 53, pp. 121-129, 2012.

[21] W. Weng, W. Hu, A. H. Dekmezian and C. J. Ruff, "Long Chian Branched Isotactic Polypropylene," *Macromolecules ,* vol. 35, pp. 3838-3843, 2002.

[22] T. Shiono, S. M. Azad and T. Ikeda, "Copolymerization of Atactic Polypropylene Macromonomer with Propene by an Isospecific Metallocene Catalyst," *Macromolecules,* vol. 32, pp. 5723-5727, 1999.

[23] E. Passaglia, S. Coiai and S. Augier, "Control of macromolecular architecture during the reactive functionalization in the melt of olefin polymers," *Progress in Polymer Science,* vol. 34, pp. 911-947, 2009.

[24] F. Romani, R. Corrieri, V. Braga and F. Ciardelli, "Monitoring the chemical crosslinking of propylene polymers through rheology," *Polymer,* vol. 43, pp. 1115-1131, 2002.

[25] M. Lazar, L. Hrckova, E. Borsig, A. Marcincin, N. Reichelt and M. Ratzsch, "Course of degradation and build-up reactions in isotactic polypropylene during peroxide decomposition," *Journal of Applied Polymer Science,* vol. 78, pp. 886-893, 2000.

[26] Y. Li, X. Xie and B. Guo, "Study on styrene-assisted melt free-radical grafting of maleic anhydride onto polypropylene," *Polymer,* vol. 42, pp. 3419-3425, 2001.

[27] C. L. Beyler and M. M. Hirschler, "Thermal decomposition of polymers," in *The SFPE handbook of fire protection engineering*, Westford, National Fire Protection Association, 2002, pp. 110-131.

[28] I. Chodak and E. Zimanyova, "The effect of temperature on peroxide initiated crosslinking of polypropylene," *European Polymer Journal,* vol. 20, pp. 81-84, 1984.

[29] M. Ratzsch, M. Arnold, E. Borsig, H. Bucka and N. Reichelt, "Radical reactions on polypropylene in the solid state," *Progress in Polymer Science,* vol. 27, pp. 1195-1282, 2002.

[30] I. Chodak and M. Lazar, "Effect of the type of radical initiator on crosslinking of polypropylene," *Die Angewandte Makromolekulare Chemie,* vol. 106, pp. 153-160, 1982.

[31] I. Chodak, K. Fabianova, E. Borsig and M. Lazar, "Crosslinking of polypropylene in the presence of polyfunctional monomer," *Die Angewandte Makromolekulare Chemie,* vol. 69, pp. 107-115, 1978.

[32] P. M. Wood-Adams, J. M. Dealy , A. W. de Groot and O. D. Redwine, "Effect of molecular structure on the linear viscoelastic behavior of polyethylene," *Macromolecules,* vol. 33, pp. 7489-7499, 2000.

[33] B. H. Zimm and W. H. Stockmayer, "The dimensions of chain molecules containing branches and rings," *Journal of Chemical Physics,* vol. 17, pp. 1301-1314, 1949.

[34] H. A. Barnes, A handbook of elementary rheology, Aberystwyth: Cambrian Printers, 2000.

[35] R. P. Lagendijk, "The influence of peroxydicarbonate modification on the extensional properties of polypropylene," Graduation Report, Delft, 1999.

[36] C. Tsenoglou and A. D. Gotsis, "Rheological characterization of long chain branching in a melt of evolving molecular architecture," *Macromolecules,* vol. 34, pp. 4685-4687, 2001.

[37] A. D. Gotsis, "Branched polyolefins," in *Applied Polymer Rheology: Polymeric Fluids With Industrial Applications*, New Jersey, John Wiley & Sons, 2012, pp. 59-112.

[38] J. M. Dealy and K. F. Wissbrun, "Dependence of viscosity on shear rate," in *Melt rheology and its role in plastic processing: Theory and applications*, New York, Van Nostrand Reinhold, 1990, pp. 159-169.

[39] F. Zulli, L. Andreozzi, E. Passaglia, S. Augier and M. Giordano, "Rheology of Long-Chain Branched Polypropylene Copolymers," *Journal of Applied Polymer Science,* vol. 127, pp. 1423-1432, 2012.

[40] J. Janzen and R. H. Colby, "Diagnosing long-chain branching in polyethylenes," *Journal of Molecular Structure,* vol. 485/486, pp. 569-584, 1999.

[41] J. M. Dealy and R. G. Larson, Structure and rheology of molten polymers; From structure to flow behavior and back again, Munchen: Hanser, 2006.

[42] D. J. Lohse, S. T. Milner, L. J. Fetters, M. Xenidou, N. Hadjichristidis, R. A. Mendelson, C. A. Carcia-Franco and M. K. Lyon, "Well-defined, model long chain branched polyethylene. 2. Melt rheological behavior," *Macromolecules,* vol. 35, pp. 3066-3075, 2002.

[43] E. C. Company, "Eastman Chemical Company," Eastman, 2013. [Online]. Available: http://www.eastman.com/Literature_Center/D/D162.pdf.

[44] A. Gandini and M. N. Belgacem, "Furans in polymer chemistry," *Progress in Polymer Science,* vol. 22, pp. 1203-1379, 1997.

[45] K. A. Kunert, J. Ranachowski, I. Chodak, H. Soszynska and N. Pislewski, "Physico-mechanical investigation of crosslinked polypropylene," *Polymer,* vol. 22, pp. 1677-1682, 1981.

[46] J. Tian, W. Yu and C. Zhou, "Crystallization behaviors of linear and long chain branched polypropylene," *Journal of Applied Polymer Science,* vol. 104, pp. 3592-3600, 2007.

[47] S. H. Tabatabaei, P. J. Carreau and A. Ajji, "Rheological and thermal properties of blends of long-chain branched polypropylene and different linear polypropylenes," *Chemical Engineering Science,* vol. 64, pp. 4719-4731, 2009.

[48] F. Su and H. Huang, "Rheological and thermal behavior of long branching polypropylene prepared by reactive extrusion," *Journal of Applied Polymer Science,* vol. 113, pp. 2126-2135, 2009.

[49] P. M. Wood-Adams and J. M. Dealy, "Using rheological data to determine the branching level in metallocene polyethylenes," *Macromolecules,* vol. 33, pp. 7481-7488, 2000.

[50] I. Chodak and M. Lazar, "Peroxide-initiated crosslinking of polypropylene in the presence of p-benzoquinone," *Journal of Applied Polymer Science,* vol. 32, pp. 5431-5437, 1986.

[51] I. Chodak, M. Lazar and M. Capla, "Crosslinking of polypropylene initiated by peroxide in the presence of thiourea as a coagent," *Journal of Applied Polymer Science,* vol. 29, pp. 581-583, 1991.

[52] E. Passaglia, P. Siciliano, F. Ciardelli and G. Maschio, "Kinetics of the free radical grafting of diethyl maleate onto linear polyethylene," *Polymer International,* vol. 49, pp. 949-952, 2000.

[53] S. Li, M. Xiao, D. Wei, H. Xiao, F. Hu and A. Zheng, "The melt grafting preparation and rheological characterization of long chain branching polypropylene," *Polymer,* vol. 50, pp. 6121-6128, 2009.

# Appendix A

| References | Peroxide | Co-agent | Additional agent |
|---|---|---|---|
| [6] | 2,5-dimethyl-2,5-(*t*-butylperoxy) hexane (DHBP) | Pentaerythritol triacrlyate (PETA) | - |
| [7] | DHBP | Trimethylol propane triacrylate (TMPTA) | 2-cyano-3-(furan-2-yl)-2-propenoic acid ethyl ester (CFA)<br><br>2-cyano-3-(thiophene-2-yl)-2-propenoic acid ethyl ester (CTA)<br><br>2-cyano-3-(pyrrole-2-yl)-2-propenoic acid ethyl ester (CPA)<br><br>2-(furan-2-ylmethylene)malononitrile (FN)<br><br>2-(thiophene-2-ylmethylene)malononitrile (TN)<br><br>2-(pyrrole-2-ylmethylene)malonitrile (PN) |
| [8] | DHBP | TMPTA | Propyl dipropyldithoicarbamate<br><br>Allyl dipropyldithiocarbamate<br><br>Benzyl dipropyldithiocarbamate |
| [9] | DHBP | TMPTA | Tetraethylthiuram disulfide (TETDS) |
| [10] | DHBP | TMPTA | TETDS<br><br>Tetramethyl thiuram disulfide (TMTDS)<br><br>Bis(piperdinothiocarbonyl) |

| | | | |
|---|---|---|---|
| | | | disulfide (BPTDS)<br><br>2,2’ dithiobis(benzothiazole) (DTBzT) |
| [11] | DHBP | PETA | - |
| [12] | Peroxydicarbonates | - | - |
| [13] | Dicumyl peroxide (DCP)<br><br>Di-4-*tert*-butylcyclohexyl peroxide (BCHPC)<br><br>Di-*tert*-butyl peroxide (DTBP)<br><br>Cumene hydroperoxide (CHP)<br><br>Dibenzoyl peroxide (BPO) | 1,6-hexanediol diacrylate (HDDA) | - |
| [14] | DHBP | TMPTA<br><br>Triallyl phosphate (TAP)<br><br>Triallyl trimesate (TAM) | - |
| [15] | DCP | TAM | - |
| [16] | BPO | 1,4-butanediol diacrylate (BDDA)<br><br>HDDA<br><br>PETA<br><br>TMPTA | - |
| [17] | DHBP | TMPTA | Fullerene ($C_{60}$) |
| [18] | DHBP | TMPTA | - |
| [19] | Peroxydicarbonates | - | - |
| [20] | DHBP | Divinylbenzene (DVB)<br><br>p-(3-butenyl)styrene (BS) | - |

# Appendix B

*Calculation of the half life time of dicumyl peroxide:*

$I \xrightarrow{k_d} 2R \cdot$

The decomposition of the peroxide is a first order reaction. Therefore we can write:

$$k_d = Ae^{\frac{-E_a}{RT}}$$

Where A is a constant (depending on the material), $E_a$ (J/mol) the activation energy, R a constant $8.314 \frac{J}{K \cdot mol}$ and T (K) the temperature.

The half life time is reached when:

$$C_t = \frac{1}{2} C_0$$

And defined according to the following equation:

$$\tau = \frac{ln\ 2}{k_d}$$

At $T_1 = 154°C (= 427\ K)$ the half life time of dicumyl peroxide is $\tau_1 = 360\ s$[6]. Therefore:

$$k_{d1} = \frac{ln\ 2}{\tau_1} = \frac{ln\ 2}{360} = 1.93 \cdot 10^{-3}\ s^{-1}$$

The activation energy, $E_a$, of dicumyl peroxide is $129.3 \cdot 10^3\ J/mol$. Now we can determine the half life time of dicumyl peroxide at 170°C (= 443 K) by dissolving the following equation:

$$\frac{k_{d1}}{k_{d2}} = \frac{e^{\frac{-E_a}{RT_1}}}{e^{\frac{-E_a}{RT_2}}} \qquad \rightarrow k_{d2} = 7.22 \cdot 10^{-3}\ s^{-1}$$

Giving the following half life time for dicumyl peroxide at 170°C:

$$\tau_2 = \frac{ln\ 2}{7.22 \cdot 10^{-3}} = 96\ s$$

[6] Defined by Akzo Nobel

# Appendix C

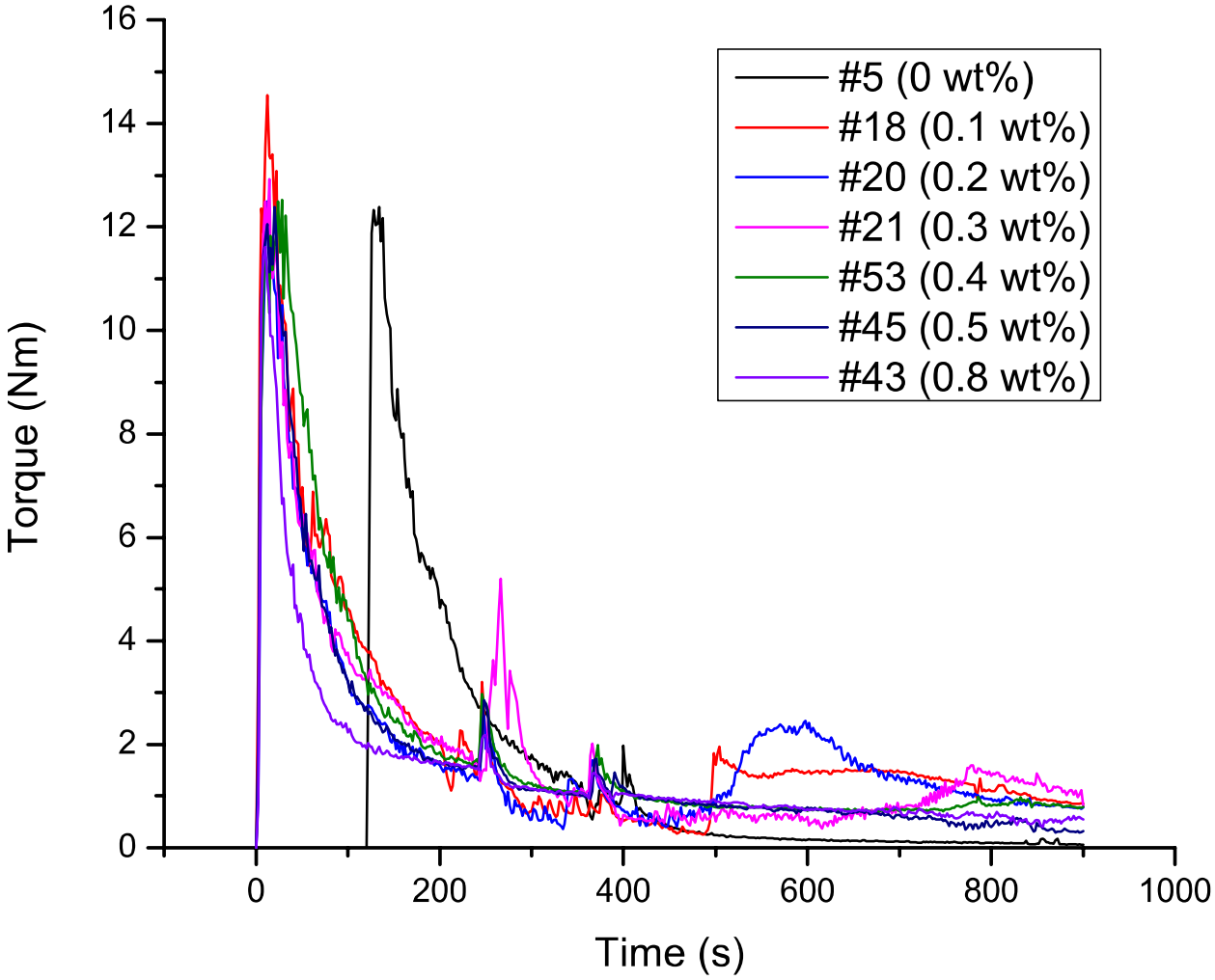


Figure 33: Behavior of the mixing torque for the samples modified with HQ

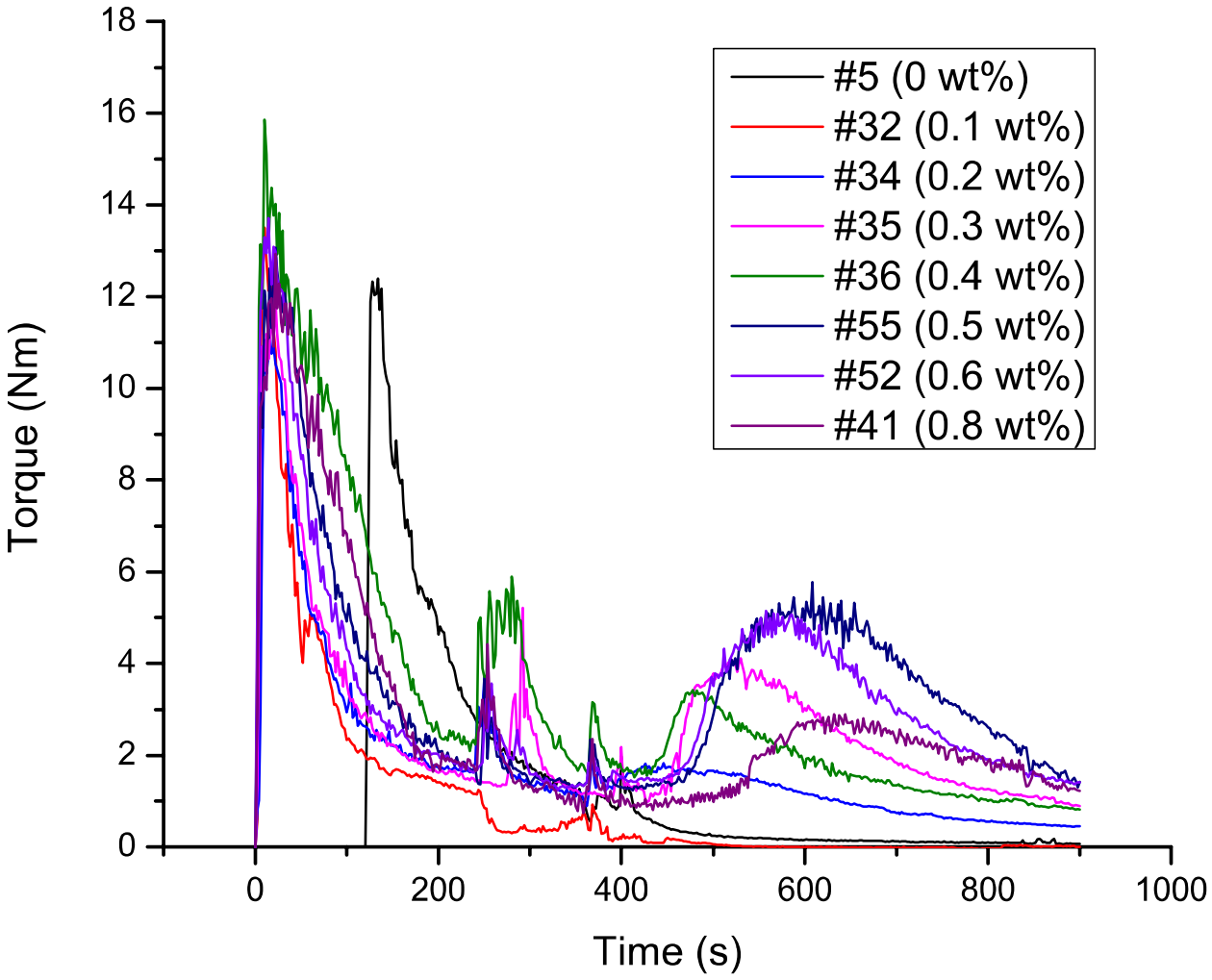


Figure 34: Behavior of the mixing torque for the samples modified with BQ

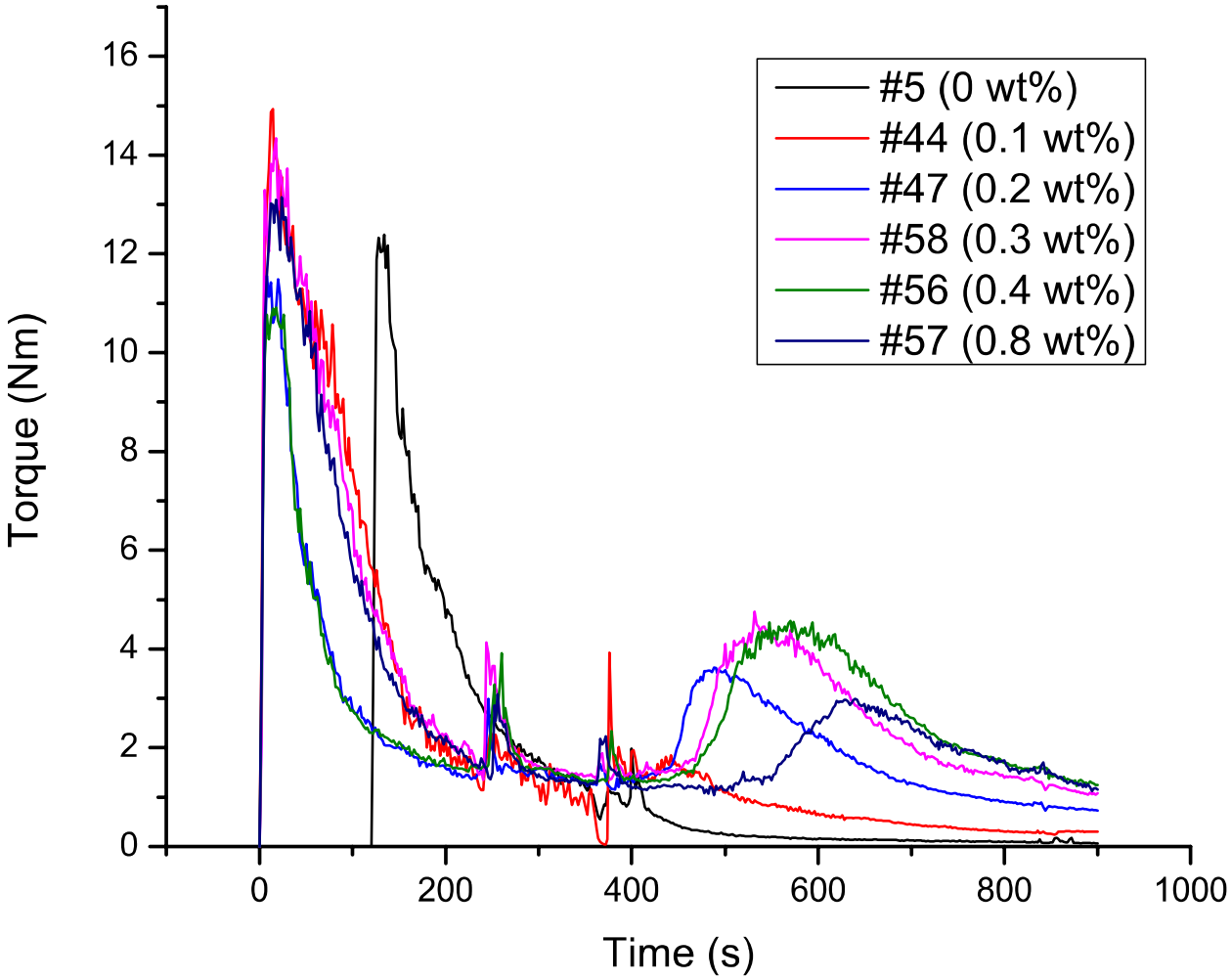


Figure 35: Behavior of the mixing torque for the samples modified with MBQ

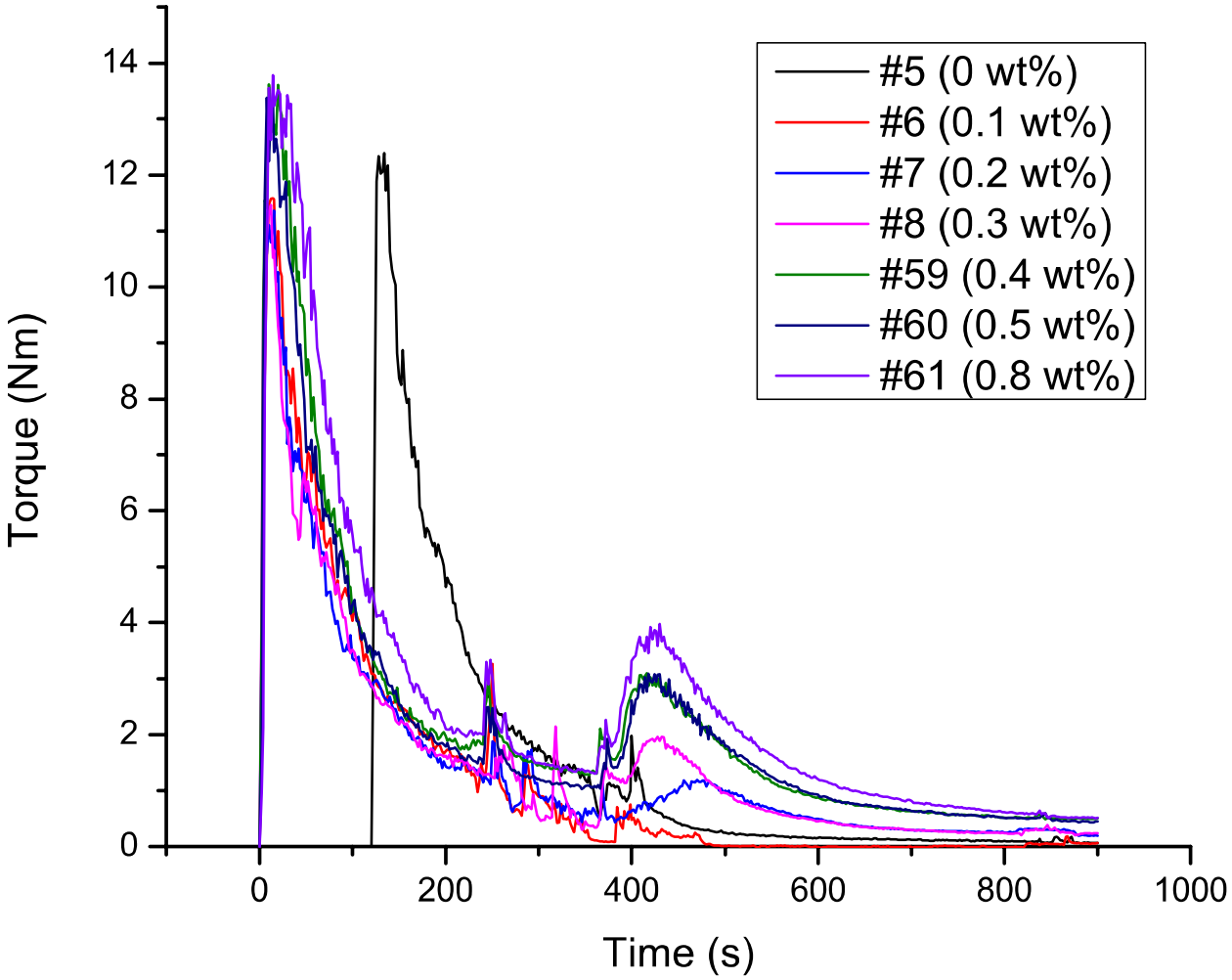


Figure 36: Behavior of the mixing torque for the samples modified with DVB

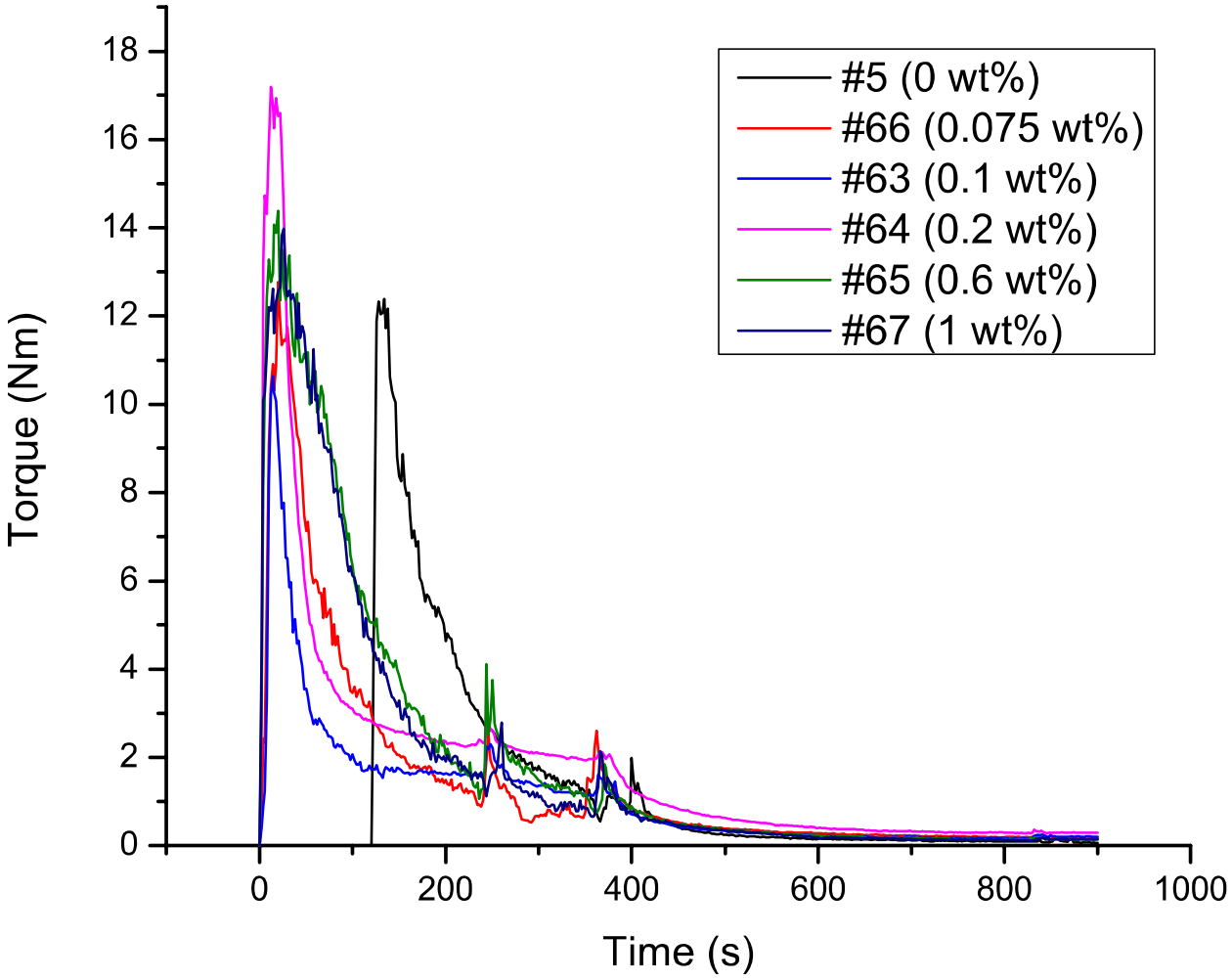


Figure 37: Behavior of the mixing torque for the samples modified with A2F